Assessing *n*-alkane and neutral lipid biomarkers as tracers for land-use specific sediment sources

C. Wiltshire [a], T.W. Waine [a,*], R.C. Grabowski [a], J. Meersmans [c], B. Thornton [b], S. Addy [b], M. Glendell [b]

[a] *School of Water, Energy and Environment, Cranfield University, Bedford MK43 0AL, United Kingdom*
[b] *The James Hutton Institute, Craigiebuckler, AB15 8QH, Aberdeen, Scotland, United Kingdom*
[c] *TERRA Teaching and Research Centre, Gembloux Agro-Bio Tech, University of Liège, Gembloux 5030, Belgium*

A B S T R A C T

Sediment fingerprinting (SF) methods using taxonomic-specific biomarkers such as *n*-alkanes have been successfully used to distinguish sediment sources originating from different land uses at a catchment scale. In this study, we hypothesise that using a combination of soil biomarkers of plant, fungal and bacterial origin may allow greater discrimination between land uses in SF studies. Furthermore, we assess if the inclusion of short chain (shorter than C22) neutral lipid fatty acids (SC-NLFA) improves land use discrimination, considering the Loch Davan catchment (34 km²) in Scotland as a case study. Fatty acids are commonly used to measure abundance and diversity of soil microbial and fungal communities. The spatial distribution of these soil communities has been shown to depend mainly on soil properties and, therefore, soil types and land management practices. The *n*-alkane and SC-NLFA concentrations and their compound specific stable isotope signatures (CSSI) in four land cover classes (crop land, pasture, forest, and moorland) were determined and their contribution to six virtual sediment mixture samples was modelled. Using a Bayesian un-mixing model, the performance of the combined *n*-alkane and SC-NLFA biomarkers in distinguishing sediment sources was assessed. The collection of new empirical data and novel combinations of biomarkers in this study found that land use can be distinguished more accurately in organic sediment fingerprinting when combining *n*-alkanes and SC-NLFA or using SC-NLFA and their CSSI alone. These results suggest that fingerprinting methods using the output of unmixing models could be improved by the use of multiple tracer sets if there is a commensurate way to determine which tracer set provides the "best" capacity for land use source discrimination. This new contribution to the organic sediment fingerprinting field highlights that different combinations of biomarkers may be required to optimise discrimination between soils from certain land use sources (e.g., arable-pasture). The use of virtual mixtures, as presented in this study, provides a method to determine if addition or removal of tracers can improve relative error in source discrimination. Combining biomarkers from different soil communities could have a significant impact on the identification of recent sources of sediment within catchments and therefore on the development of effective management strategies.

1. Introduction

Fine grained sediment is a natural and important component of fluvial systems, however, increased fluxes can impact stream ecological health and river functioning (Owens et al., 2005; Scheurer et al., 2009; Stenfert Kroese et al., 2020). Catchment soils contribute to a wide range of ecosystem services and fulfil many roles including structural and resources, filter and reservoir, fertility and biodiversity and climate regulation (Dominati et al., 2010; McBratney et al., 2014). Natural processes such as erosion and the loss of soil carbon can be greatly accelerated by changes in climate and human activity (Battin et al., 2009; Gobin et al., 2004; Koch et al., 2013), resulting in increased lateral fluxes of soil organic carbon (SOC) to waterways. Therefore, it is of vital importance to identify sources of sediment within catchments to inform effective management strategies.

Sediment fingerprinting has emerged in the last 20 years as an

essential approach to quantify the relative contribution of different land use sources to organic matter load in waterways (Alewell et al., 2016; Chen et al., 2017; Glendell et al., 2018; Hancock and Revill, 2013; Liu et al., 2021b; Walling et al., 1999). However, broad land use classifications (e.g., agricultural land cover, natural land cover) do not enable precise SOC origins to be determined or, consequently, management strategies to be targeted (Owens et al., 2016). The use of multiple source group classifications (e.g., cropland, pasture, forest, moorland) can result in a greater spatial resolution of sediment origin, however, each of the sources must be discriminated strongly by at least one tracer. In consequence, the more source groups used, the more unlikely it will be that sufficiently strong discriminators are available for all sources (Collins et al., 2020; Pulley and Collins, 2018).

Fingerprinting methods using taxonomic-specific tracers (e.g. *n*-alkane ratios) (Galoski et al., 2019; Glendell et al., 2018; Liu et al., 2021a; Zhang et al., 2017) and compound-specific stable isotope (CSSI) signatures of long-chain (longer than C22) fatty acids (LCFAs) (Alewell et al., 2016; Hirave et al., 2020b), have been successfully applied to distinguish sediment sources originating from different land uses at a catchment scale. The *n*-alkanes are widely used plant biomarkers (Bush and McInerney, 2013). These naturally occurring unbranched hydrocarbons are an important constituent of cuticular plant leaf-waxes, deposited in soil by leaf-fall, and are relatively resistant against degradation (Zech et al., 2011). The *n*-alkanes are stable, long-lived molecules that can survive in the fossil record for millennia (Bush and McInerney, 2013). This has led to their use as biomarkers in tracing vegetation input to soil and sediments over decadal and centennial time scales (Chen et al., 2017, 2022; Glendell et al., 2018; Wang et al., 2015) and also in paleoecology and paleoclimatology (Glaser and Zech, 2005; Meyers, 2003; Zech et al., 2009). The longer the *n*-alkane chain length, the less soluble they are in water, reducing their metabolism by microorganisms (Cranwell, 1981; Ranjan et al., 2015). Consequently, alkanes of chain-length >C24 are generally resistant to biodegradation (Singh et al., 2012) making them suitable as conservative sediment tracers. Plants produce a range of *n*-alkanes with a strong odd-over-even predominance (OEP) and one or two dominant chain lengths: trees and shrubs are characterised by C27 or C29, grass is characterised by C31 or C33 (Bush and McInerney, 2013; Meyers, 2003; Zech et al., 2013) and lower plants and mosses by C23 and C25. Short-chain length *n*-alkanes (<C23) are typically derived from aquatic algae (Ficken et al., 2000; Meyers, 2003). Variability in the carbon isotopic signatures (δ^{13}C) of *n*-alkanes is driven both by plant physiology/biochemistry and environmental factors (e.g. temperature, humidity, isotopic composition of water/CO_2) and is therefore (theoretically) unique for each individual plant and able to differentiate between different land cover types (Cooper et al., 2015 and references therein). However, as tracers such as *n*-alkanes can persist in sediments for decades to centuries (Smeaton et al., 2021), the "fingerprint" for a specific land use can be considered to reflect both past and present biomarkers at a particular site and moment. Consequently, due to agricultural rotation, arable land and temporary grassland may end up with similar signatures (Upadhayay et al., 2017). Tracing the fate of terrestrial to aquatic fluxes of sediment can be further complicated by the direct deposition, storage and degradation of plant or woody OC in the streams and rivers from which the sediment samples are taken, masking the signature from any eroded terrestrial soil (Wiltshire et al., 2022). Combining soil tracers of plant, fungal and bacterial origin may allow greater discrimination between land uses and provide a fingerprint more characteristic of the soil rather than the current land cover vegetation.

Microbial communities have the potential to identify sediment derived from different land use activities (Zhang et al., 2016b). Soil microbial communities directly affect soil functioning through cycling of soil nutrients and carbon storage and, as the spatial distributions of soil microbial communities have been shown to depend mainly on soil properties (Xue et al., 2018), it is likely that microbial communities will also represent the heterogeneity in soil type and land cover. Short chain

(defined in this study to be shorter than C22) neutral lipid fatty acids (SC-NLFA) can be of microbial or fungal rather than plant origin. Neutral lipid molecular biomarkers such as iso- and anteiso-C15:0 fatty acid methyl esters (bacterial origin) can persist in soils for decades and have proved to be effective in distinguishing land uses (Lavrieux et al., 2012). Previous studies have shown that C16 and C18 length fatty acids can distinguish crop-specific signatures (Blake et al., 2012), that fatty acids, considered common to prokaryotic and eukaryotic organisms, were particularly relevant for land use discrimination (Ferrari et al., 2015) and that lipid composition can show the effects of catchment land use on particulate OM in streams (Lu et al., 2014). SC-NLFA also show the potential to distinguish between historic land uses although their residence time in soils is not certain. Whereas Swales and Gibbs (2020) found it took around 6 years for the new land use to overwrite the earlier land use fingerprint, Lavrieux et al. (2012) were able to distinguish two reference soil profiles developed under grassland and forest vegetation from a former grassland soil converted to forest about 60 years previously. The potential for SC-NLFA to distinguish between historical land uses opens the potential for improved source attribution and commensurately, a need to verify any improvement. Artificial and virtual mixtures of known source soil proportions have been successfully used to test or validate different fingerprinting methods and models, or test the accuracy of apportioning methods (Fatahi et al., 2022; Gibbs, 2008; Lizaga et al., 2019; Palazón et al., 2015). They could, therefore, provide a basis for selecting tracers that can deliver more accurate source discrimination and apportionment.

This study: i) uses multiple types of biomarkers (*n*-alkane ratios and SC-NLFA) and their CSSIs to estimate the proportional contribution of land use sources to streambed sediment mixtures and ii) explores the use of virtual mixtures to determine if addition or removal of tracers can improve relative error in source discrimination. Soil samples from four land uses from a Scottish catchment (Loch Davan) were used i) as sources to generate virtual sample mixtures and ii) to characterise the sources for SF. The catchment has four major land uses (arable, pasture, forest and moorland) which are all potential sources of sediment within catchment streams. The aims of this study were to i) use virtual mixtures and a Bayesian un-mixing model to determine which combination of tracers provided the best capacity for land use source discrimination by reproducing known source apportionments and ii) use the best set of tracers to estimate the proportional contribution of each land use to the catchment streambed sediments.

2. Material and methods

2.1. Study site

The Dee is a major river in north-east Scotland whose catchment covers an area of about 2100 km^2 on predominantly Precambrian metamorphic and igneous rocks. The Dee flows for over 130 km from its headwaters in the Cairngorms and reaches the North Sea on Scotland's east coast at Aberdeen. The Dee catchment is a designated Special Area of Conservation (SAC) due to the presence of species such as freshwater pearl mussel, Atlantic salmon and otter (https://sac.jncc.gov.uk/site/UK0030251) and is an important source of drinking water (Jenkins, 1985). Loch Davan is a shallow (mean depth 1.2 m) throughflow lake located within the Muir of Dinnet National Nature Reserve (NNR) and drains through Davan Burn to the River Dee between Ballater and Aboyne (Jenkins, 1985). The main water input to Loch Davan is via Logie Burn and its feeder streams, and derives primarily from over-land surface flows (Smith et al., 2018a). Loch Davan's catchment covers an area of ca. 34 km^2 in which Logie Burn and its feeder streams drain a variety of land uses including higher elevation moorland (29%) and forest (22%: a mix of commercial woodland consisting of Scots pine, Norway spruce and Sitka spruce and semi-natural sparse native birch, rowan, alder and pine) and arable (10%) and pasture (31%) at lower elevation (Fig. 1b). The catchment reaches a maximum elevation in the
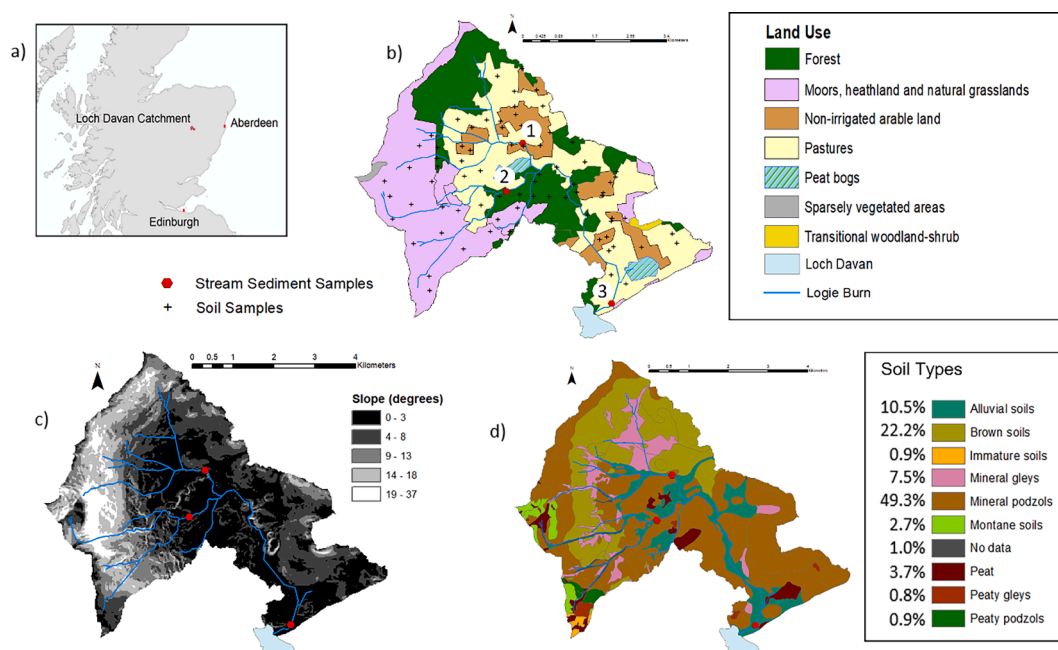
Fig. 1. Loch Davan study catchment. a) Study catchment location, b) Land use of the Loch Davan catchment (34 km^2), suspended and streambed sediment sampling locations (red dots. Sites 1, 2 and 3, referred to as BS1, BS2 and BS3) and terrestrial soil sampling locations (black crosses),based upon Corine land cover 2012 for the UK, Jersey and Guernsey (Cole et al., 2015), c) catchment slope (degrees) derived from OS Terrain 5 © Crown copyright and database rights 2021 Ordnance Survey (100025252)(Ordnance Survey, 2021), d) Catchment soils based on "1:25,000 Hutton Soils Data" copyright and database right The James Hutton Institute (2018). Used with the permission of The James Hutton Institute. All rights reserved.

west (750 m a.s.l.) gradually decreasing to the east and south to a minimum at Loch Davan (165 m a.s.l.). Areas of steepest slope (13–37°: Fig. 1c) are found under moorland and forest land cover to the west and north-west of the catchment, with arable and pasture land cover dominating the relatively flat (typically <3°slope) lowlands. The catchment mean annual precipitation is 780 mm with average annual minimum temperature of 3.5 °C and average annual maximum temperature of 12.2 °C (Met Office, 2021). The major soil types observed in the catchment are mineral podzols (49%), brown soils (22%), and alluvial soils (11%) with around 5% of soils being peat or peaty gleys/podzols ("1:25,000 Hutton Soils Data" copyright and database right The James Hutton Institute (2018); Fig. 1d). The lake area of Loch Davan has been significantly reduced over the last century, likely due to inputs of nutrient rich sediment due to land use intensification (Addy et al., 2012); between 2007 and 2018, the loch and its main feeder stream, Logie Burn, were classified as having poor to moderate ecological status (SEPA, 2021).

2.2. Sample collection

In this study, a field campaign was carried out in June 2019 to collect soil and sediment samples within the Loch Davan catchment and Logie Burn stream network. Soil samples from four land uses (arable, pasture, forest and moorland) were collected to characterise potential sediment sources for SF. Streambed samples were collected at three locations to estimate the proportional contribution of each of the land use source to

the streambed sediments in two tributaries and a joint outlet (Fig. 1b).

2.2.1. Source sampling

Replicate soil samples were taken to characterise each of the four land uses arable (n = 16), forest (n = 16), moorland (n = 18) and pasture (n = 19) at sites shown with a cross (+) in Fig. 1b. Sampling sites were chosen on the basis of likely hydrological connectivity and were stratified by land use and soil type (Table 1). For each sampling point, three replicates were chosen at random within a 2 m radius. Each sample was taken with a steel cylinder (6 cm depth and 6 cm diameter) and litter was removed before taking the sample. All samples were georeferenced by using a GPS device (horizontal accuracy sub-meter real-time), stored in plastic bags and freeze-dried on return to the laboratory. The samples were then passed through a 2 mm sieve to remove stones and larger organic material before being ground. A composite sample was formed for each site by adding an equal weight of each of the three finely ground samples. Samples were stored in sealed containers at room temperature until required for analysis.

2.2.2. Streambed sampling

Bed sediment samples were taken at 3 locations (Fig. 1b), representing two tributaries and a joint outlet. The locations were carefully chosen above their joint junction in the stream network so the contributions from each tributary could be assessed. Logie Burn originates in two main headwaters (Fig. 1) with the northern most branch (BS1) supporting similar cover of pasture (30%), forest (29%) and moorland

Table 1
Number of soil samples taken for each land use and soil type combination.

	Alluvial soils	Brown soils	Mineral gleys	Mineral podzols	Peaty gleys	Peaty podzols	No data	Montane soils	Total
arable	2	3	2	9	0	0	0	0	16
forest	2	2	2	10	0	0	0	0	16
moorland	3	4	4	3	1	1	1	1	18
pasture	4	3	4	7	1	0	0	0	19
Total	11	12	12	29	2	1	1	1	

(28%) with around 10% arable land. The western branch (BS2) predominantly passes though moorland (78%) with around 14% of the land use being pasture, <5% forest and no arable land. A third site (BS3) was located close to the outlet of Logie Burn to Loch Davan integrating input from the whole catchment. At each site three samples of bed sediments were taken with a steel cylinder (6 cm depth and 6 cm diameter) along a transect across the streambed and composited. All samples were georeferenced using GPS, stored in plastic bags and freeze-dried on return to the laboratory. The samples were then passed through a 2 mm sieve to remove stones and larger organic material before being ground and stored at room temperature until further analysis.

2.3. Laboratory analysis

2.3.1. Extraction of n-alkanes

To isolate the hydrocarbon fraction of the samples for analysis, total lipid extraction was followed by lipid fractionation (Dove and Mayes, 2006). For quality and quantification control purposes, 50 μl of alkane standard solution (docosane (C_{22}) and tetratriacontane (C_{34}) in decane) was added to the samples prior to extraction. First 3 ml of 1 M Ethanolic KOH solution was added to each sample in a tube before they were capped and heated for 16 h at 90 °C in a dry-block heater. The following steps were then repeated twice: 3 ml heptane was added to each tube which were capped and swirled before 1 ml of deionised water was added and the tubes re-capped and shaken vigorously; after separation into two liquid layers, the top (non-aqueous) layer was transferred to a new glass tube. The resulting solution was evaporated to dryness on a dry-block heater fitted with a sample concentrator blowing nitrogen (N_2) into the tube. The resultant was re-dissolved in 0.3 ml heptane with warming before transferring the sample to SPE-Si cartridge, adding 2 ml heptane and collecting the elution in a 1.5 ml autosampler vial. Solution in the vial was then evaporated to dryness.

2.3.2. Extraction of NLFAs

The samples (5–10 g) were analysed by lipid extraction with a single phase chloroform mixture before fractionation on a SPE Si column and mild methanolysis. The solvents chloroform and methanol (1:2) were used in lipid extraction and, in addition, 0.15 M of citrate buffer (0.8:1:2 of citrate buffer: chloroform: methanol (Bligh and Dyer (B&D) solvent ratio)). 15–20 ml B&D solvent was added to the sample in a glass media bottle (closed using PTFE lined cap) which was then sonicated for 30 min (in ultrasonic bath). This was followed by centrifuge at 700 RCF for 10 min before the upper layer was poured into a clean glass media bottle. Chloroform (4 ml) and citrate buffer (4 ml) were added before centrifuging at 700 RCF for 10 min. Successful separation was indicated by both layers appearing clear and the upper (aqueous) layer was aspirated and discarded leaving the bottom organic layer. The glass bottle was then placed in an evaporator at 37 °C and dried under N_2.

The neutral lipids were then separated from the lipid extract by fractionation (Solid Phase Extraction (SPE)). SPE columns were prepared with ~0.5 g anhydrous sodium sulphate (Na_2SO_4) and chloroform before the lipid extracts were added along with 1 ml chloroform. Five ml of chloroform was used to elute the neutral lipids (sterols). These were collected in a clean glass bottle placed in an evaporator at 37 °C and dried under N_2 for 4–5 h. To quantify the subsequently produced FAMEs an internal standard, 60 μl of C19:0 methyl ester (Methyl nonadecanoate in methanol: 25 mg/l) was added to the dried phospholipid fraction after SPE and evaporated to dryness under N_2.

The samples were then methylated by adding 1 ml of toluene: methanol (1: 1) (stored on Na_2SO_4) and 1 ml of 0.56 g potassium hydroxide in 50 ml methanol to the neutral lipid fraction (NLF). This was swirled and incubated @37 °C for 30 min. Subsequently, 0.25 ml of acetic acid 59 ml l^{-1}, 5 ml of hexane:chloroform (4: 1)(v/v) and 3 ml deionised water were added and the NLF glass bottle was centrifuged at 700 RCF for 10 min. The upper organic phase was collected in a Gilson pipettor and the lower aqueous phase discarded. The resultant liquid

was dispensed through 10 ml pipette tip packed with glass-wool and Na_2SO_4 into clean glass bottle and rinsed with a few ml of hexane. The glass bottle was placed in an evaporator at 20–25 °C and dried under N_2. The dried FAMEs were then stored in a freezer at −20 °C.

2.3.3. Analysis of n-alkanes and FAMES by GC-C-IRMS

Individual *n*-alkane and FAMEs were quantified and their δ^{13}C values determined by GC-C-IRMS using a Trace GC Ultra gas chromatograph (Thermo Finnigan, Bremen, Germany) equipped with a GC PAL autosampler (CTC Analytics AG, Zwingen, Switzerland) following the method described in Thornton et al., (2011).

2.3.4. Quality control and assurance

The apportionment of upstream sources of the river sediments used relative rather than absolute concentrations of both alkanes and neutral lipids. An assumption was made that the percentage recovery of individual alkanes was similar and correspondingly that of individual neutral lipids was similar.

For both *n*-alkanes and neutral lipids, every batch of samples extracted contained a solvent blank taken through the extraction procedure which allowed assessment of any potential contamination issues; none being observed. Additionally, a quality control soil sample was also extracted with each sample batch. Typical concentration values for the quality control soil were for the alkane tetracosane (C24) 0.50 ± 0.07 nmoles g^{-1} soil (mean ± sd, n = 5) and for the lipid 18:1w7 = 135 ± 6 nmoles g^{-1} soil (mean ± SD, n = 8).

For δ^{13}C analysis by GC-C-IRMS, reference materials, run with every sample batch, with certified δ^{13}C values were used to normalise the δ^{13}C values of the neutral lipids and alkanes onto the VPDB scale. The reference materials used were Hexadecanoic acid methyl ester (C16:0) #1 (δ^{13}C = −30.74 ‰) and Icosanoic acid methyl ester (C20:0) #Z3 (δ^{13}C = −1.54 ‰) for neutral lipids and Hexacosane (C26) #2 (δ^{13}C = –32.94 ‰) for alkanes. All reference materials were obtained from the Schimmelmann laboratory Indiana University. Long term monitoring, over several months, of Nonadecanoic acid methyl ester (C19:0) used as a quality control material gave δ^{13}C values of −30.6 ± 0.6 ‰ (mean ± SD, n = 160).

2.4. n-alkane and SC-NLFA tracers

2.4.1. n-alkanes

The *n*-alkane concentrations and δ^{13}C were obtained for carbon chain lengths C21 to C38 where δ^{13}C is defined as:

$$\delta 13C = R(13C/12C)_{sample}/R(13C/13C)_{ref} - 1 \qquad (1)$$

where $R(^{13}C/^{12}C)_{sample}$ and $R(^{13}C/^{12}C)_{ref}$ are the absolute isotope ratios of a sample and the reference material (in this case - Vienna PeeDee Belemnite) respectively.

The data was sub-set (Fig. 2a) to include only those biomarkers that were present in all soil and sediment samples. This sub-set included carbon chain lengths C23-C31 from which ratios were then calculated for use as tracers: the relative percentage of *n*-alkanes C27, C29 and C31 (Torres et al., 2014); the C27 to C31 ratio (Puttock et al., 2014); P_{aq}, to understand aquatic versus terrestrial plant input (Ficken et al., 2000); the Odd-to-Even Predominance (OEP) (Zech et al., 2013; and the Average Chain length (ACL) (Fang et al., 2014) (Table 2).

2.4.2. SC-Nlfa

Seven of the 36 SC-NLFA biomarkers analysed in this study were found in both streambed sediments and all terrestrial soil samples: i15:0, a15:0, 16:0, 10-Methyl-16:0, 12-Me-16:0, 18:2ω6,9, and 18:0. The relative concentration of these seven SC-NLFA was then obtained by dividing the measured concentration by the sum of all concentrations.
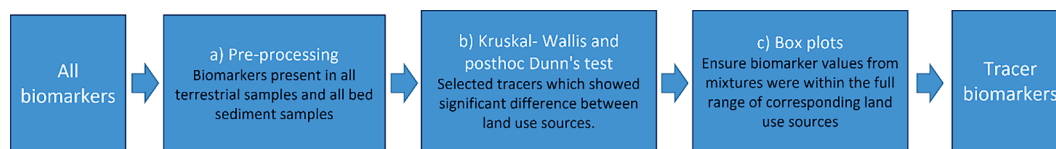
Fig. 2. Summary of tracer selection methodology.

Table 2
N-alkane ratios considered as tracers for land use discrimination.

n-alkanes ratios	Indicative of:	Reference
C_{27}/C_{31} $\%Ci = \dfrac{Ci}{(C27 + C29 + C31)}$ $Paq = \dfrac{C23 + C25}{C23 + C25 + C29 + C31}$ $OEP = \dfrac{C27 + C29 + C31}{C26 + C28 + C30}$ $ACL =$ $\dfrac{25 \times C25 + 27 \times C27 + 29 \times C29 + 31 \times C31}{C25 + C27 + C29 + C31}$	C27 to C31 ratio estimating the proportion of wood to grass derived organic matter % of alkane "i" Relative contribution of higher aquatic vs. terrestrial plants Organic matter degradation: odd-over-even predominance (OEP) Average chain length (ACL) - weight-averaged number of carbon atoms of the higher plant C_{25}–C_{31} n-alkanes	(Puttock et al., 2014) (Torres et al., 2014) (Ficken et al., 2000) Adapted from (Zech et al., 2013) Adapted from (Jeng, 2006)

2.4.3. Tracer selection

Tracers should i) discriminate between all the potential sediment sources and, (ii) be conservative (remain stable during transport and deposition (Collins et al., 2020; Hirave et al., 2020a)). Tracer values of all source (land use) groups were first checked for normal distribution using the Kolmogorov-Smirnov test. A Kruskal- Wallis (KW) and posthoc Dunn's test was then carried out to select tracers which showed significant differences between land use sources (Fig. 2b). The tracers which passed the KW test were then assessed using box plots (Excel) to ensure biomarker values from all mixtures were within the full range of corresponding land use sources (Fig. 2c). In addition, $\delta^{13}C$ biomarker tracers were only selected if their corresponding concentration values were within the range of stream sediment mixtures (Collins et al., 2020). The full range (excluding outliers) was used for the range test as, according to Bayesian inference, best practice suggests comparison of full distributions for hypothesis testing (Fenton and Neil, 2018). The streambed sediment mixtures are represented by a single measurement without any knowledge of the potential mean and distribution. This single measurement could represent a value close to the maximum or minimum of the possible tracer values rather than the mean and therefore selecting tracers based solely on the means and inter-quartile range of the sources was considered too restrictive.

Unless otherwise stated, all MixSIAR runs, statistical and error analyses were carried out in R (version 3.6.3) (R Core Team, 2020) and RStudio (version 1.1.463) (RStudio Team, 2018).

2.5. Bayesian unmixing model (MixSIAR) implementation

The MixSIAR model was first developed for ecological studies but is increasingly being applied in catchment sediment fingerprinting research (Lachance et al., 2020; Smith et al., 2018b; Stenfert Kroese et al., 2020). Tracer properties can be characterised using the mean and standard deviation and the model is fitted using Markov chain Monte Carlo (MCMC). Source means and standard deviations used in the mixture likelihood are allowed to deviate from user specified values with the amount of deviation dependent on source sample sizes. A full description of this model can be found in Stock and Semmens (2016) and Stock et al. (2018).

Running MixSIAR using isotopic tracers provides the proportional contribution of the sources to the isotopic tracer in the mixture. As it is the proportional contribution of the sources to the sediment mixture which is of interest here, the MixSIAR model was run as concentration dependant taking into account differences in the concentration of

individual isotopic tracers (here *n*-alkanes or FAs) (Upadhayay et al., 2018). Sediment source proportions were estimated using 3000 MCMC simulations with MixSIAR formulated using a process error term (no residual error), an uninformative prior and three chains. Initially for each run the MCMC parameters were set to those for a "normal" run with chain length = 100,000, burn = 50,000, thin = 50. The Gelman-Rubin and Geweke diagnostic tests were used to evaluate convergence of all models (Stock and Semmens, 2016). Regarding the Gelman-Rubin, in each case none of the variables were >1.01 indicating that the between chain variance was small, chains were mixing around the stationary distribution and longer burn-in was not required. For cases where the Geweke diagnostic indicated individual chains were not convergent, the model was run again with MCMC parameters progressively set to those for a "long" run (chain length = 300,000, burn = 200,000, thin = 100), "very long" run (chain length = 1,000,000, burn = 500,000, thin = 500) and in rare cases "extreme" run (chain length = 3,000,000, burn = 1,500,000, thin = 500) until all chains converged (Stock and Semmens, 2016).

2.6. Virtual mixtures

Land use discrimination was assessed using "virtual" mixtures with 50/50 contributions from each of the four sources (arable, pasture, forest and moorland) by taking the mean of two sources to represent a 50% contribution from each (Collins et al., 2020). This resulted in six virtual 50/50 mixtures: Arable-Forest (AF50), Arable-Moorland (AM50), Arable-Pasture (AP50), Forest-Moorland (FM50), Forest-Pasture (FP50) and Moorland-Pasture (MP50). Errors were calculated as mean absolute differences between the modelled and virtual mixture composition.

3. Results and discussion

3.1. n-alkane ratios

Plants produce a range of *n*-alkanes with a strong odd-over-even predominance (OEP) and one or two dominant chain lengths: trees and shrubs are characterised by C27 or C29, grass is characterised by C31 or C33 (Bush and McInerney, 2013; Meyers, 2003; Zech et al., 2013) and lower plants, macrophytes and mosses by C23 and C25. Surprisingly, C31 was the most abundant homologue in arable, moorland and forest land (Fig. 3). The relative proportions of the homologues were very similar in arable and forest soils giving them a very similar *n*-alkane
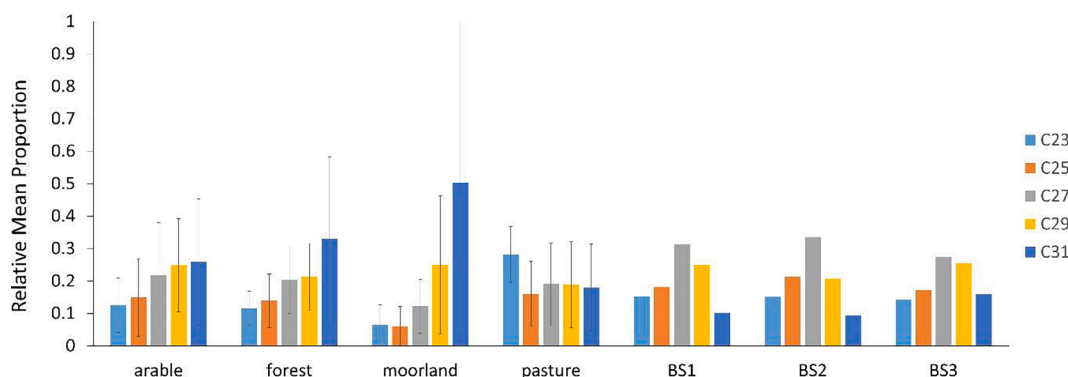
Fig. 3. Relative mean proportions for mid and long-chain n-alkane homologues for the soils of land uses, arable, forest, moorland, and pasture and streambed sediments BS1, BS2 and BS3. Where present, error bars +/- 1SD.

signature. The moorland and pasture soil n-alkane signatures were more distinctive with moorland dominated by C31 and pasture land surprisingly dominated by C23 with a relatively small contribution from C31 (even though C31 is usually dominant in grassland). It is possible that, in this catchment, pastures are located in wetter areas with more mosses contributing to higher C23 abundance. In contrast, the bed sediment n-alkane signatures (BS1, BS2 and BS3) reach a peak for the C27 and C29 homologues with relatively smaller contributions from C31.

The values of the n-alkane proxy for aquatic versus terrestrial plant input (P_{aq}) were similar in arable and forest soils (0.38 ± 0.15 and 0.35 ± 0.17 respectively), higher in pasture soils and streambed sediments (0.58 ± 0.12 and 0.43 to 0.55, respectively) and lower in moorland soils (0.18 ± 0.14) (Table 3; Fig. 4). These values for P_{aq} are larger than those ascribed by Ankit et al. (2022) to terrestrial vegetation (<0.1) and actually lie predominantly in the range attributed to emergent macrophytes ($0.1–0.4$) (Ankit et al., 2022). Although, it seems unlikely that aquatic macrophytes would make a significant contribution to terrestrial soils across the catchment, their presence could account for the relatively higher P_{aq} and C23/C25 contribution in streambed sediments and possibly in pasture soils if these are located in wetter areas. Although the differences in P_{aq} between soil types were not significant (Kruskal-Wallis p < 0.05), alluvial soils (recent riverine and lacustrine alluvial deposits) showed a relatively larger P_{aq} (Fig. 5). The number of soils samples taken on alluvial soils for each land use (Table 1: arable 2 of 16 = 12.5%; forest 2 of 16 = 12.5%; moorland 3 of 18 = 17% and pasture 4 of 19 = 21%) is unlikely to account for the differences in P_{aq} seen for those land uses as moorland and pasture had similar percentages of alluvial soil samples but had the lowest and highest values of P_{aq} respectively.

OEP is often used as a measure of organic matter degradation with

lower OEPs indicative of higher degradation (Zech et al., 2013). Stout (2020) found the OEP was relatively lower for soil compared to the less degraded leaves/litter and in addition found preferential and progressive degradation of the more abundant C27/C29 homologues relative to the less abundant C31/C33 from fresh leaves, through litter to the corresponding soil; the %C31 was relatively higher for soil compared to the less degraded leaves/litter. In this study, the OEP values of both streambed sediments and pasture soils were much smaller than those in arable, forest or moorland soils, which could suggest that they were more degraded. However, their corresponding %C31, which (particularly for the bed sediments) are relatively lower would suggest the opposite. The n-alkane ratios for alluvial soils had significantly larger % C27 and lower %C31 than other soil types (Fig. 5). The range of values for these ratios seen in the alluvial soil type was similar to that seen in streambed sediments which also showed relatively large %C27 and lower %C31. Light soil fractions can exhibit relatively higher amounts of mid-chain n-alkanes with low CPI values compared to bulk soil (Carbon preference index (CPI) is another n-alkane ratio proxy for the predominance of odd over even, similar to OEP) (Griepentrog et al., 2016). As finer sediments are more likely to be mobilised during water run-off than coarser sediments (Sirjani et al., 2022), sediments reaching the streams could be derived primarily from the finer fraction of terrestrial soils. This finding could account for the relatively large proportions of n-alkanes C25-C29 compared to C31 (Fig. 3) as well as the low OEP values (Fig. 4) seen in streambed sediments.

Although contribution from aquatic macrophytes/lower plants and mosses could account for the relatively higher C23/C25 (and P_{aq}) contribution in streambed sediments, equally elevated values were found in pasture soils. A larger input of pasture soil (relative to other land uses) to streambed sediments could account for their relatively higher C23/C25. When studying emergent aquatic plants, He et al. (2020) found that long chain n-alkanes (e.g., C29) were predominantly derived from leaves rather than roots in wetland surface sediments/soils, but the contribution from mid-chain n-alkanes (e.g., C23) from roots may be equal to or greater than those from leaves. Griepentrog et al. (2016) also found the relative abundance of n-alkanes differed depending on the specific origin of the OM. For forest vegetation, they found root biomass was characterized by a higher relative abundance of mid-chain n-alkanes ($<$C26) and low CPI, whereas leaves had much higher CPI since they consisted almost exclusively of C27 and C29. Therefore, if a similar characterisation of the relative abundance of n-alkanes is found in pasture vegetation, a larger contribution of n-alkanes from roots rather than leaves could be contributing to relatively higher C23 abundance in pasture soils. It is possible this could be driven by the preferential removal of leaf material by grazers.

The ranges of n-alkane ratios in streambed sediments were outside the maximum and minimum values for the land use sources for C27/C31 and %C31 (Fig. 4). The difference in range between the streamed

Table 3
Mean (+/- 1SD) values of n-alkane ratios for forest, pasture, arable and moorland land uses and streambed sediment sources (BS1, BS2 and BS3).

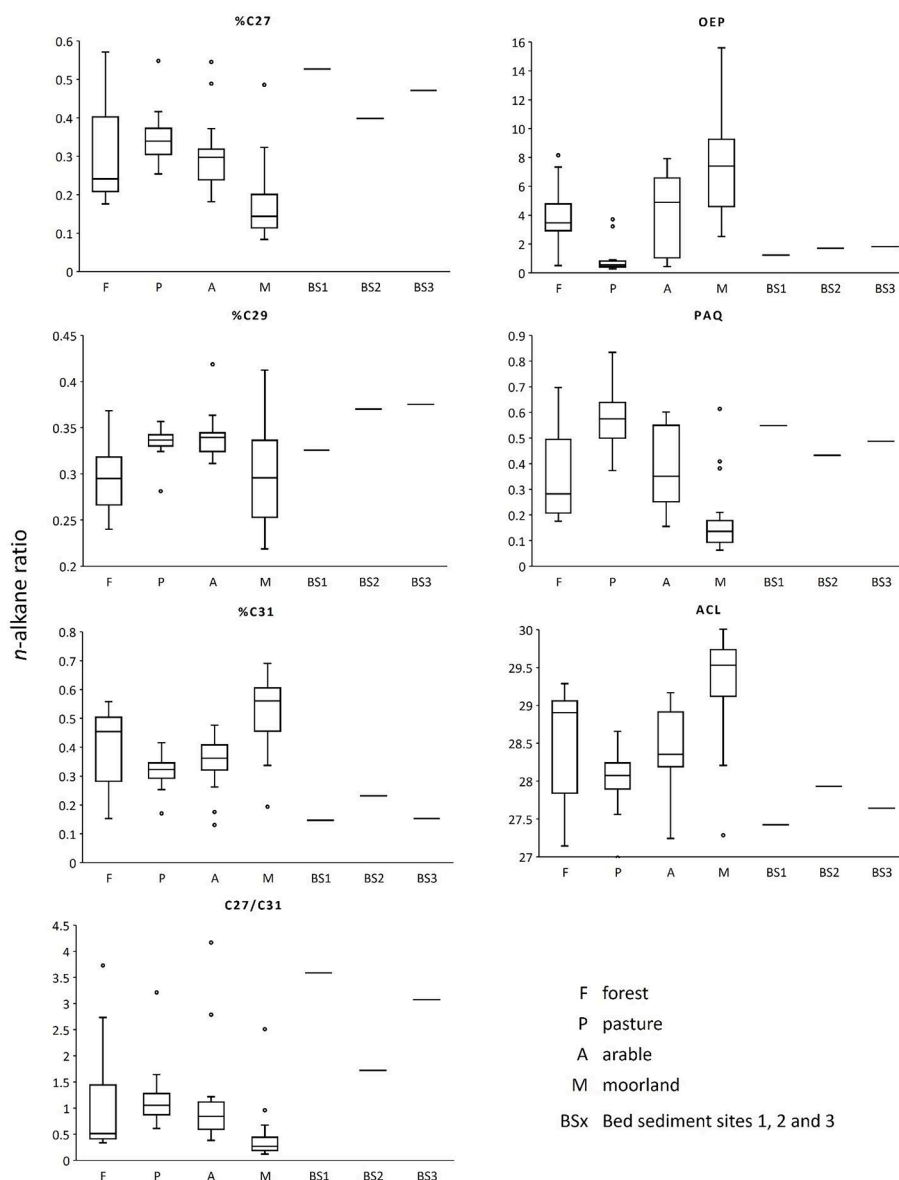|	C27/C31	%C27	%C29	%C31	OEP	P_{aq}	ACL
arable (16)	1.10 ± 0.99	30.63 ± 9.65	34.10 ± 2.54	35.27 ± 9.69	4.26 ± 2.72	0.38 ± 0.15	28.38 ± 0.55
forest (16)	1.02 ± 1.01	29.90 ± 12.78	29.42 ± 3.56	40.68 ± 13.02	3.76 ± 2.09	0.35 ± 0.17	28.55 ± 0.74
moorland (18)	0.45 ± 0.56	17.60 ± 9.95	30.24 ± 5.53	52.17 ± 12.63	7.22 ± 3.40	0.18 ± 0.14	29.34 ± 0.66
pasture (19)	1.20 ± 0.55	35.07 ± 6.26	33.55 ± 1.62	31.38 ± 5.20	0.87 ± 0.93	0.58 ± 0.12	28.03 ± 0.36
BS 1	3.59	52.73	32.56	14.70	1.23	0.55	27.42
BS 2	1.72	39.83	37.02	23.15	1.71	0.43	27.93
BS 3	3.08	47.13	37.54	15.32	1.82	0.49	27.64

Fig. 4. Range of n-alkanes ratios C27/C31, %C27, %C29, %C31, OEP, P_{aq} and ACL from forest, pasture, arable and moorland land uses and streambed sediment sources. The box is extended from the 25–75 percentiles, the line is plotted at the median and whiskers show the maximum to minimum range excluding outliers (dots).

sediment *n*-alkanes and those of the terrestrial land uses was primarily due to the relatively lower and higher %C31 and %C27 respectively in the streambed sediments which commensurately reduced the average chain length (ACL) and increased the C27/C31 ratio (Table 3). On average, pasture soils also showed a lower and higher %C31 and %C27 relative to the other land uses, respectively (Table 3), however, the smallest %C31 and largest %C27 and ratios were found in forest soils (Fig. 4). Within a forest environment, both leaves and needles show increased C27/C31 ratio compared with soil, with C27 being particularly dominant in leaves. Hence, the higher C27/C31 ratio seen in forest soil samples could be due to a higher contribution of less degraded leaves/needles or litter (Griepentrog et al., 2016). An input of less degraded leaves/needles or litter could also account for the relatively high C27/C31 ratio found in streambed sediments. However, the relatively higher %C31 of less degraded leaves/litter would also be accompanied by a corresponding increase in OEP (Stout, 2020), which was not observed in streambed sediments in this study. An alternative explanation could be related to bacterial sources of *n*-alkanes, with distribution patterns ranging from C11 to C35 often without

an increase in OEP (Ladygina et al., 2006). A microbial *n*-alkane pool could be responsible for mid and long-chain *n*-alkanes with low OEP in leaf litter samples (Zech et al., 2011). Grimalt et al. (1988) found that, when sediments from a previously freeze-dried core were stored under water for a month, the *n*-alkane profiles previously ranging between C25 and C33 with high OEP were transformed into mixtures of C22-C29 *n*-alkanes with negligible OEP. They suggested this could be due to microbial transformations either due to *n*-alkane sources of bacterial origin, or to the re-working of organic matter by bacteria. Increased presence or activity of microbes due to the presence of water could account for the lower presence of long-chained *n*-alkanes (C31) and low OEP in the streambed sediment samples and possibly in the alluvial soils. The low OEP and relatively low %C31 seen in pasture soils cannot be directly linked with water sources and are interspersed with arable land throughout the catchment (Fig. 1b). However, soil sampling sites were chosen on the basis of likely hydrological connectivity with the streams, i.e. located on accumulated flow lines, so these locations could be expected to support high soil moisture content. However, this explanation is confounded by the fact that similar reduction in OEP was not observed
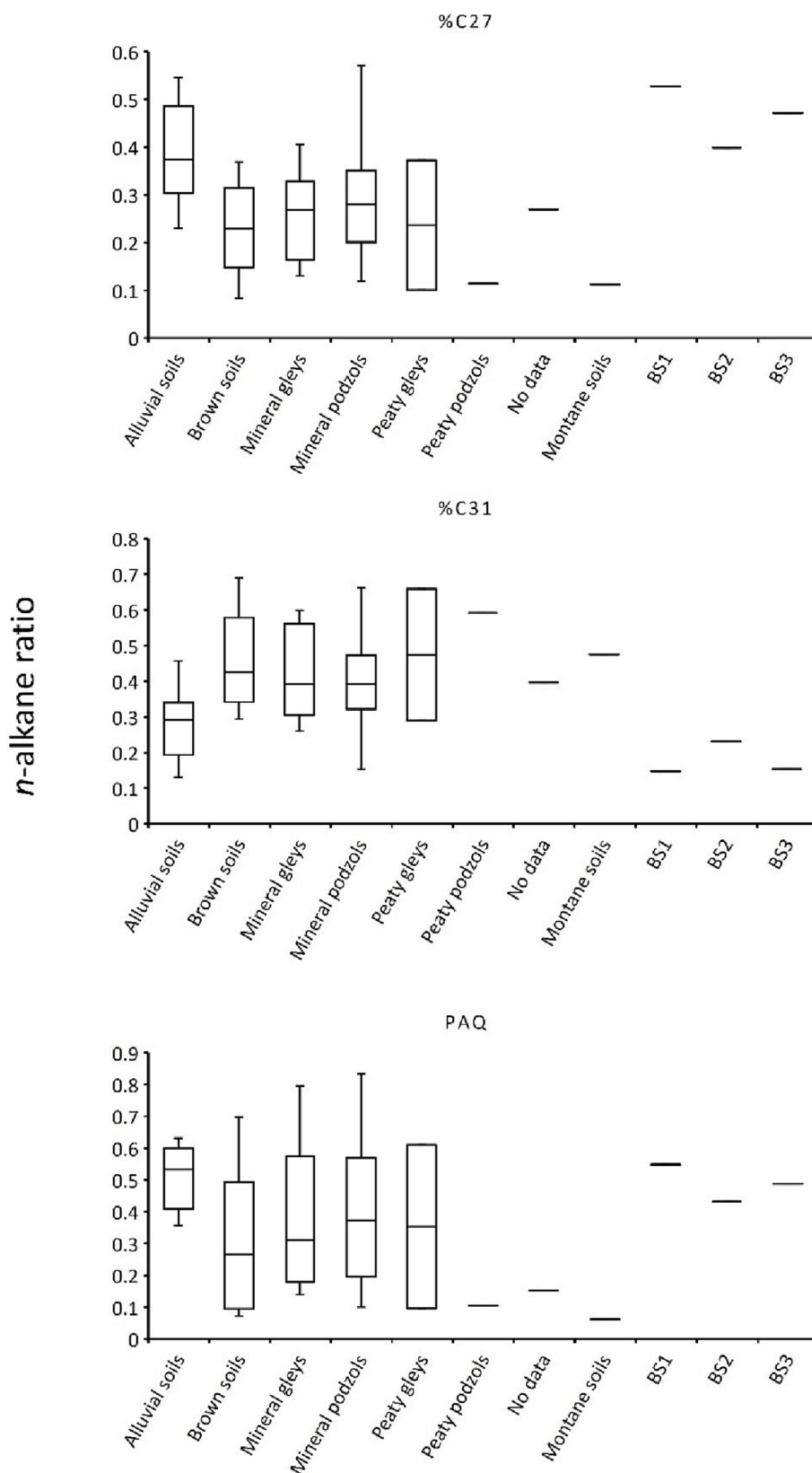
Fig. 5. Range of n-alkanes ratios %C27 and %C31 from different soil types (Alluvial, Brown soils, Mineral Gleys, Mineral Podzols, Peaty Gleys, Peaty Podzols and Montane soils) and streambed sediment sources BS1, BS2 and BS3 The box is extended from the 25–75 percentiles, the line is plotted at the median and whiskers show the maximum to minimum range excluding outliers.

in samples taken in other land uses, which were also preferentially located in hydrologically well-connected locations.

In summary, the *n*-alkane values of the streambed sediments are similar to the forest soils in terms of their lower %C31 and higher %C27 values and similar to the pasture soils in their low OEP. Tracer conservativeness relies on these characteristics having the same source, that is, the high C27/C31 and low OEP are due to the presence of forest soil and pasture soil respectively in the streambed sediments and not significantly to the direct input of leaves/litter and/or microbial transformations as discussed above. As the streambed sediment mixtures are represented by a single measurement without any knowledge of the potential mean and distribution, the single measurement could represent a value close to the maximum or minimum of the possible tracer values rather than the mean. Although in this study three bed samples were taken across the burn and combined (yielding a single measurement) to have a representative stream sample, it is still possible changes occur within relatively short distances up- or downstream and therefore it is recommended in future fingerprinting studies to take a larger number of samples to represent the streambed sediments. In addition, the conservativeness of tracers is always of concern in fingerprinting studies and there is a reliance on the assessment of corresponding soil and sediment tracers ranges. In future studies, an assessment of variation in biomarkers at different stream hydromorphological locations (near-bank, channel centre, behind a log-jam etc.) might allow some assessment of in-stream (non-soil) tracer sources. In this way, the stream sediments could be more reliably compared with those of the terrestrial sources. More confidence that *n*-alkane ratios in the streambed sediments show the same range as the land use soils would lead to more confidence in rejecting alternative sources for streambed OC. The following tracer selection was carried out on the assumption that any tracer for which all streambed sediment samples fell within the full range of corresponding land use sources could be classed as conservative.

3.1.1. Tracer selection

All *n*-alkane ratios showed significant differences between land use sources (Table 4). The ranges of C27/C31 and %C31 ratios in streambed sediments were outside the maximum and minimum values for the land use sources (Fig. 4). Hence the remaining five *n*-alkane ratios (%C27, %C29, OEP, P_{aq} and ACL) were selected as tracers. Individually, only OEP and P_{aq} ratios could discriminate between most land uses, however together, these five biomarkers could discriminate between all land cover class combinations (Table 4). To distinguish four land use sources, a minimum of three tracers is required (Phillips and Gregg, 2003). The availability of five conservative *n*-alkane biomarkers confirms they could be used to provide a baseline scenario against which *n*-alkane and SC-NLFA biomarker combinations could be compared.

3.2. n-alkane CSSI $\delta^{13}C$

Five of the 18 CSSI $\delta^{13}C$ biomarker signatures measured in this fingerprinting study were detected in both streambed sediments and all terrestrial soil samples (C23, C25, C27, C29 and C31). The range of *n*-alkane CSSI $\delta^{13}C$ values in the soil samples and streambed sediment samples were all within those typical of *n*-alkanes in C3 land plants (ca. 39-30‰ (Chikaraishi and Naraoka, 2003)) except for C23 which showed less depleted values in both terrestrial samples (arable, forest and moorland) and streambed sediment samples BS1 and BS2. However, some of the streambed sediment CSSI $\delta^{13}C$ signatures for C25, C27 and C29 chain lengths were less negative than, and outside the maximum and minimum values for, the land use sources (Fig. 6). In their study of peat deposits, Yan et al. (2021) revealed preferential degradation under aerobic conditions of mid-chain *n*-alkanes relative to their long-chain homologs (C29 and C31), resulting in an increase in both the relative proportions of long-chain *n*-alkanes and less depleted $\delta^{13}C$ values of mid-chain *n*-alkanes. However, it seems unlikely that this is the cause of the less depleted $\delta^{13}C$ values of C25-C29 *n*-alkanes in the streambed sediments in this study, as relative proportions of *n*-alkanes C25-C29, indicative of lower plants and woody material, are greater than the longer chain C31, indicative of grasslands (Fig. 3). Alternatively, Wang et al. (2016) study of *n*-alkanes in fine and coarse particle fractions of surface peat revealed that $\delta^{13}C$ values of odd-numbered *n*-alkanes (C23–C33) were generally less negative in the finer fraction. They attributed the less negative $\delta^{13}C$ to greater heterotrophic reworking during degradation within the finer fractions compared to the coarser fraction. If finer sediments were preferentially mobilised during water run-off, sediment reaching the streams may derive primarily from the finer fractions of the terrestrial soil (Nitzsche et al., 2022; Sirjani et al., 2022).

3.2.1. Tracer selection

All the CSSI $\delta^{13}C$ in the soil samples were found to distinguish between land uses (Table 5). However, the CSSI $\delta^{13}C$ biomarker signatures for C25, C27 and C29 were outside the maximum and minimum values for the land use sources (Fig. 6). Hence, only C23 and C31 CSSI signatures were selected as tracers and, together, these two biomarker signatures discriminated between all land cover class combinations except between arable and forest, and moorland and forest (Table 5). The availability of only two conservative *n*-alkane CSSI $\delta^{13}C$ biomarker signatures meant that they could not be used on their own to distinguish between four land use sources in this catchment and would not be able to discriminate well between forest land cover and either arable or moorland.

3.3. SC-NLFA concentrations

Seven of the 36 SC-NLFA biomarkers analysed in this study were detected in both streambed sediments and all terrestrial soil samples: i15:0, a15:0, 16:00, 10-Methyl-16:0, 12-Me-16:0, 18:2ω6,9, 18:00. Of these, all SC-NLFA relative concentrations (with the exception of 16:00) could distinguish between land uses (Table 6). Biomarkers a15:0 and 12-Me-16:0 were outside the maximum and minimum values for the land use sources and, therefore, only four SC-NLFA biomarkers (i15:0, 10-Methyl-16:0, 18:2ω6,9 and 18:00) were selected as tracers (Fig. 7). Together, these four biomarkers could discriminate between all land cover class combinations except arable and pasture (Table 6).

Iso 15:0 (i15:0) is a biomarker for gram-positive bacteria and has been used to study trophic relationships in soil food webs (Haubert et al., 2006) and 10-Methyl-16:0 is characteristic of actinomycetes (Tekaya et al., 2021). Actinomycetes are particularly abundant in soils, especially in alkaline soils and soils rich in organic matter, where they form an important part of the microbial population (Barka et al., 2016; Zaitlin et al., 2003). Large numbers of actinomycetes enter freshwater from land with soil runoff (Zaitlin et al., 2003). NLFA 18:2ω6,9 is present in
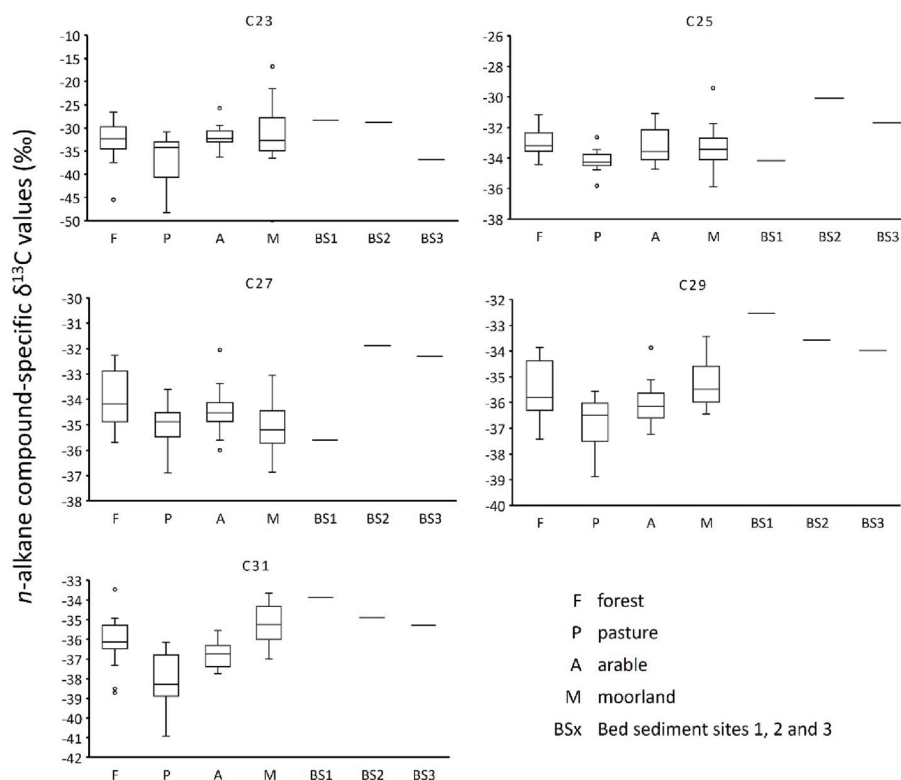
Table 4
Kruskal- Wallis (KW) and posthoc Dunn's test: significant differences in n-alkane ratios (p < 0.05) distinguished between soil samples from different land use sources. Sources in bold indicate n-alkane ratios for streambed sediment within the range for terrestrial sediments.

	Significant difference (p < 0.05)						
	C27/ C31	% C27	% C29	% C31	OEP	P_{aq}	ACL
Arable-Forest			√				
Arable-Moorland	√	√	√	√		√	√
Arable-Pasture					√	√	
Forest-Moorland	√	√			√	√	√
Forest-Pasture			√	√	√	√	
Moorland-Pasture	√	√	√	√	√	√	√

Fig. 6. Range of δ¹³C values (‰) of n-alkanes (C23-C31) from forest, pasture, arable and moorland land uses and streambed sediment sources The box is extended from the 25–75 percentiles, the line is plotted at the median and whiskers show the maximum to minimum range excluding outliers (dots).

Table 5
Kruskal- Wallis (KW) and posthoc Dunn's test. significant differences in n-alkane CSSI δ¹³C (p < 0.05) distinguished between soil samples from different land use sources. Sources in bold indicate n-alkane CSSI δ¹³C value for streambed sediment within the range for terrestrial sediments.

	Significant difference (p < 0.05)				
	C23	C25	C27	C29	**C31**
Arable-Forest					
Arable-Moorland					√
Arable-Pasture	√	√			
Forest-Moorland			√		
Forest-Pasture		√	√	√	√
Moorland-Pasture		√		√	√

plant storage lipids and is the dominant fatty acid in most fungi (Olsson et al., 2005). Within a forest environment Ferlian et al., (2014) found the fungal biomarker 18:2ω6,9 was more abundant in litter as compared to soil whereas the opposite was true of bacterial biomarkers such as i15:0 which were more abundant in the soil.

The relative mean proportions of SC-NLFA i15, 10-Methyl-16, 18:2ω6, and 18:0 for forest soil samples were very different from

samples from other land uses (Fig. 8) with roughly equal contributions from all four biomarkers (i15:0 0.32, 10-Methyl-16:0 0.22, 18:2ω6,9 0.21 and 18:0 0.25). Arable and moorland show a similar signature dominated by the fungal biomarker 18:2ω6,9 (0.5 and 0.59 respectively) with correspondingly smaller contributions from the bacterial bio-markers i15:0 and 10-Methyl-16:0 (combined proportion of 0.18 and 0.19 respectively) and biomarker 18:0 (0.32 and 0.22 respectively) ubiquitous in both bacteria and plants. The relative mean proportions of SC-NLFA in pasture land soil samples had a larger contribution from the bacterial biomarkers i15:0 and 10-Methyl-16:0 (combined proportion of 0.29) than those in arable/moorland soils and a correspondingly smaller proportion from the fungal biomarker 18:2ω6,9 (0.37). The study of Zaitlin et al. (2003) found actinomycetes are particularly abundant in runoff from terrestrial sources with faecal contamination, suggesting an increased contribution of bacterial biomarkers in pasture land relative to arable or moorland could be due to the presence of grazing animals. It is not known why bacterial biomarkers dominate the distribution in forest soils, however, bacterial and fungal communities can vary with nutrient availability and particle size fractions (Hemkemeyer et al., 2019; 2018; Zhang et al., 2016a) contributing to spatial heterogeneity and bacterial diversity between land uses. There is a relatively larger proportion bacterial biomarkers in the streambed sediments (BS1 0.29, BS2 0.45,

Table 6
Kruskal- Wallis (KW) and posthoc Dunn's test. significant differences in Neutral lipid fatty acid (NLFA) relative concentration (p < 0.05) distinguished between soil samples from different land use sources. Sources in bold indicate NLFA concentrations for streambed sediment within the range for terrestrial sediments.

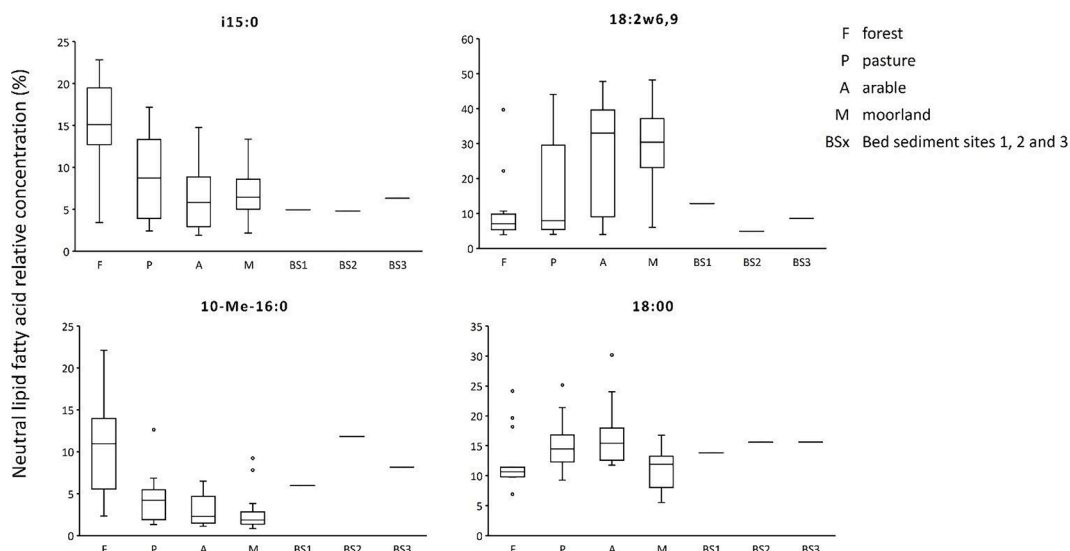|	Significant difference (p < 0.05)						
	i15:0	a15:0	**16:0**	**10-Methyl-16:0**	12-Methyl-16:0	**18:2ω6,9**	**18:0**
Arable-Forest	√			√		√	√
Arable-Moorland					√		√
Arable-Pasture							
Forest-Moorland	√	√		√	√	√	
Forest-Pasture	√			√			√
Moorland-Pasture		√			√	√	√

Fig. 7. Range of SC-NLFA i15:0, 10-Methyl-16:0, 18:2ω6,9 and 18:00 from forest, pasture, arable and moorland land uses and streambed sediment sources BS1, BS2 and BS3. The box is extended from the 25–75 percentiles, the line is plotted at the median and whiskers show the maximum to minimum range excluding outliers (dots).
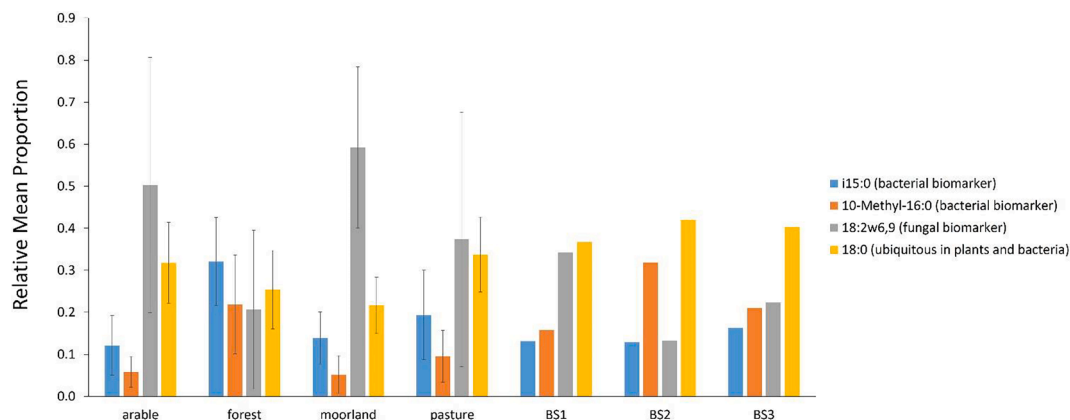

Fig. 8. Relative mean proportion for SC-NLFA for the soils of land uses, arable, forest, moorland and pasture streambed sediments BS1, BS2 and BS3. Error bars +/- 1SD.

and BS3 0.37) relative to most of the land uses (arable 0.18, moorland 0.19, pasture 0.29 and forest 0.54). The sample site for BS2 is within an area of forest and it is possible bank overflow or erosion could have provided a larger contribution from forest soils to streambed sediments at this site. Alternatively, the range of $\delta^{13}C$ of *n*-alkanes suggested streambed sediments could have relatively more finer soil particles, and in the study of Hemkemeyer et al. (2018) actinobacteria were shown to exhibit preference for the fine silt particle fraction.

3.4. SC-NLFA CSSI $\delta^{13}C$

CSSI $\delta^{13}C$ signatures of conservative SC-NLFAs (selected above) (i.e., i15:0, 16:00, 10-Methyl-16:0, 18:2ω6,9 and 18:00) (Table 7) were considered as potential tracers. Of these, all SC-NLFA CSSI $\delta^{13}C$ (with the exception of 16:00) could distinguish between land uses (Table 7). The CSSI $\delta^{13}C$ values for i15:0 and 18:2ω6,9 were outside the maximum and minimum values for the land use sources and therefore only 10-Methyl-16:0 and 18:00 were selected as tracers (Fig. 9). Together, these biomarkers could only discriminate between forest land and the other three land uses (Table 7). The availability of only two conservative SC-NLFA CSSI $\delta^{13}C$ biomarkers and their ability to distinguish a limited number of land use classes meant that they could not be used on their

Table 7
Kruskal- Wallis (KW) and posthoc Dunn's test: significant differences in NLFA CSSI $\delta^{13}C$ ($p < 0.05$) distinguished between soil samples from different land use sources. Sources in bold indicate NLFA CSSI $\delta^{13}C$ for streambed sediment within the range for terrestrial sediments.

	Significant difference ($p < 0.05$)				
	i15:0	16:00	**10-Methyl-16:0**	18:2ω6,9	**18:00**
Arable-Forest			√	√	
Arable-Moorland					
Arable-Pasture					
Forest-Moorland			√		
Forest-Pasture	√		√	√	√
Moorland-Pasture	√				

own to distinguish between the four land use sources in this catchment.

3.5. Combination of tracers that provided the best land use source discrimination

Six "virtual" mixtures with 50/50 contributions from each of the four sources (arable, pasture, forest and moorland) were created to test the
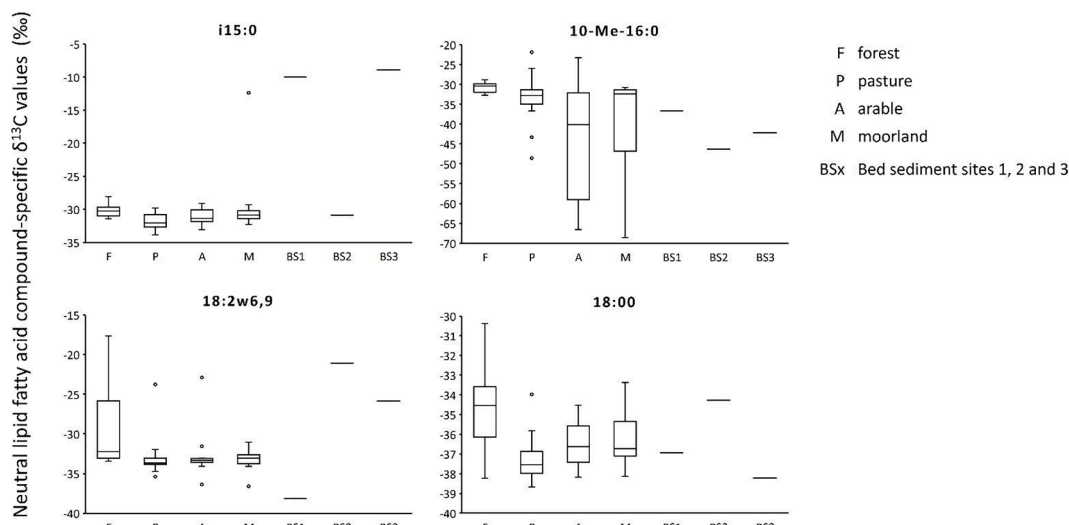
Fig. 9. Range of δ¹³C values (‰) of SC-NLFA from forest, pasture, arable and moorland land uses and streambed sediment sources The box is extended from the 25–75 percentiles, the line is plotted at the median and whiskers show the maximum to minimum range excluding outliers (dots).

performance of MixSIAR in distinguishing between land uses when using the following tracer combinations; Scenario a) *n*-alkane ratios alone (Nalk), b) *n*-alkane ratios + CSSI signatures (NalkBoth), c) *n*-alkane ratios + SC-NLFA concentrations (NalkNlfa), d) Scenario c + SC-NLFA CSSI signatures (NalkNlfaBoth), e) SC-NLFA concentrations only (Nlfa), f) SC-NLFA concentrations + CSSI signatures (NlfaBoth), and g) all tracers (Fig. 10, Table 8).

If the "best" tracer set is defined as minimising the error when distinguishing between land use sources, then using Scenario e (SC-NLFA concentrations (Nlfa); four biomarkers in total) was the best in distinguishing arable or forest land use from all other land use sources (4.3% and 3.7% mean error respectively) (Table 8). The best tracer set in distinguishing pasture land from all other land uses was Scenario f (SC-NLFA concentrations + CSSI signatures (NlfaBoth)). Using a combination of *n*-alkane ratios + SC-NLFA concentrations (NalkNlfa) was the best tracer set to distinguish moorland from all other land uses (Table 8). To distinguish between all four land uses the best tracer set was Scenario f (SC-NLFA concentrations + CSSI signatures (NlfaBoth)) (Table 8). If the "worst" tracer set is defined as the maximum error when distinguishing between land use sources, then Scenario b *n*-alkane ratios + CSSI signatures (NalkBoth) was the worst tracer set to distinguish between the four land uses in this catchment. When distinguishing between all four land uses the minimum error was found by not using any *n*-alkane

Table 8

Mean absolute difference between modelled and virtual mixture composition (%) for Scenario a) n-alkane ratios alone (Nalk), b) n-alkane ratios + CSSI signatures (NalkBoth), c) n-alkane ratios + SC-NLFA concentrations (NalkNlfa), d) Scenario c + SC-NLFA CSSI signatures (NalkNlfaBoth), e) SC-NLFA concentrations only (Nlfa), f) SC-NLFA concentrations + CSSI signatures (NlfaBoth), and g) all tracers. Land use 50/50 combinations: Arable-Forest (af), Arable-Moorland (am), Arable-Pasture (ap), Forest-Moorland (fm), Forest-Pasture (fp) and Moorland-Pasture (mp). "Best" tracer set is defined as minimising the error when distinguishing between land use sources and is highlighted in green.

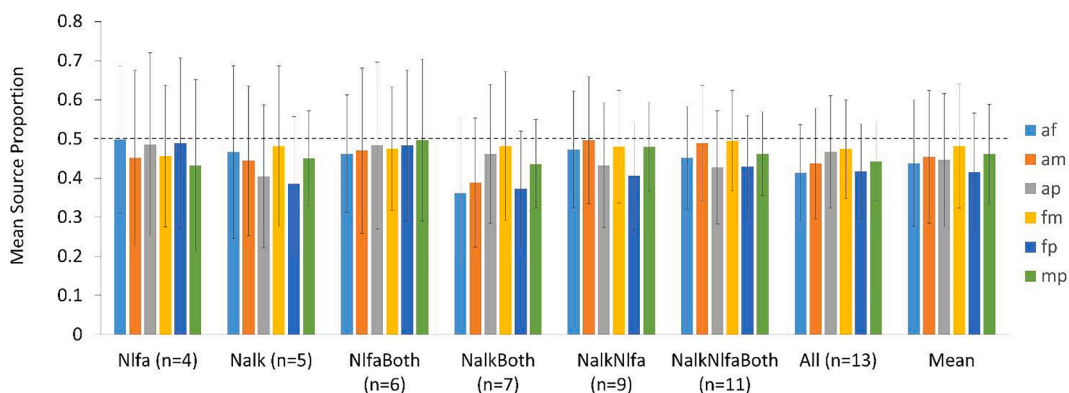|	arable (mean of af, am, ap)	forest (mean of af, fm, fp)	pasture (mean of ap, fp, mp)	moorland (mean of am, fm, mp)	All land uses
Nlfa	4.27	3.73	6.27	10.80	6.27
Nalk	12.40	11.20	17.40	8.33	12.33
Nlfa both	5.67	5.33	2.47	3.87	4.33
NalkBoth	19.27	19.07	15.33	13.00	16.67
NalkNlfa	6.60	9.47	12.27	3.00	7.83
NalkNlfaBoth	8.87	8.33	12.13	3.60	8.23
All	12.20	13.07	11.60	9.80	11.67
Mean all tracer sets	9.90	10.03	11.07	7.49	

Fig. 10. Source proportions modelled for 50/50 virtual mixtures for Scenario a) n-alkane ratios alone (Nalk), b) n-alkane ratios + CSSI signatures (NalkBoth), c) n-alkane ratios + SC-NLFA concentrations (NalkNlfa), d) Scenario c + SC-NLFA CSSI signatures (NalkNlfaBoth), e) SC-NLFA concentrations only (Nlfa), f) SC-NLFA concentrations + CSSI signatures (NlfaBoth), and g) all tracers. Land use 50/50 combinations. Arable-Forest (af), Arable-Moorland (am), Arable-Pasture (ap), Forest-Moorland (fm), Forest-Pasture (fp) and Moorland-Pasture (mp). Dotted line at proportion of 0.5 (50/50). Error bars +/- 1SD. n = number of tracers.

tracers in the MixSIAR source apportionment. For this catchment, where discrimination between four different land uses is required, the combined use of SC-NLFA concentrations + CSSI signature tracers (Nlfa-Both) provided the best capacity for land use source discrimination based on the reproduction of known source apportionments. Distinguishing between arable and pasture land using *n*-alkane tracers is known to be difficult due to agricultural rotation (Glendell et al., 2018; Wiltshire et al., 2022). These results suggest that the addition of SC-NLFA tracers to *n*-alkanes or the use of SC-NLFA tracers alone could improve the discrimination between these two land uses.

In previous studies, soil fungal community structures under afforestation have been shown to be controlled by original land use practices (Xue et al., 2022) and soil biomarkers of bacterial origin have proved to be effective, not only in distinguishing current land uses, but also in distinguishing soil under land that had changed use decades before (e.g. grassland to forest (Lavrieux et al., 2012)). Combining SOC biomarkers from different soil communities may allow future studies to achieve even more accurate SOC source attribution using multiple source group classifications based not just on the current land use but on known conversions of land use (e.g., cropland to forest). For example, if SC-NLFA could distinguish former grassland under afforestation from existing forest and grasslands these tracers could be used to see the effect of this land use change on the sources of sediments in nearby streams.
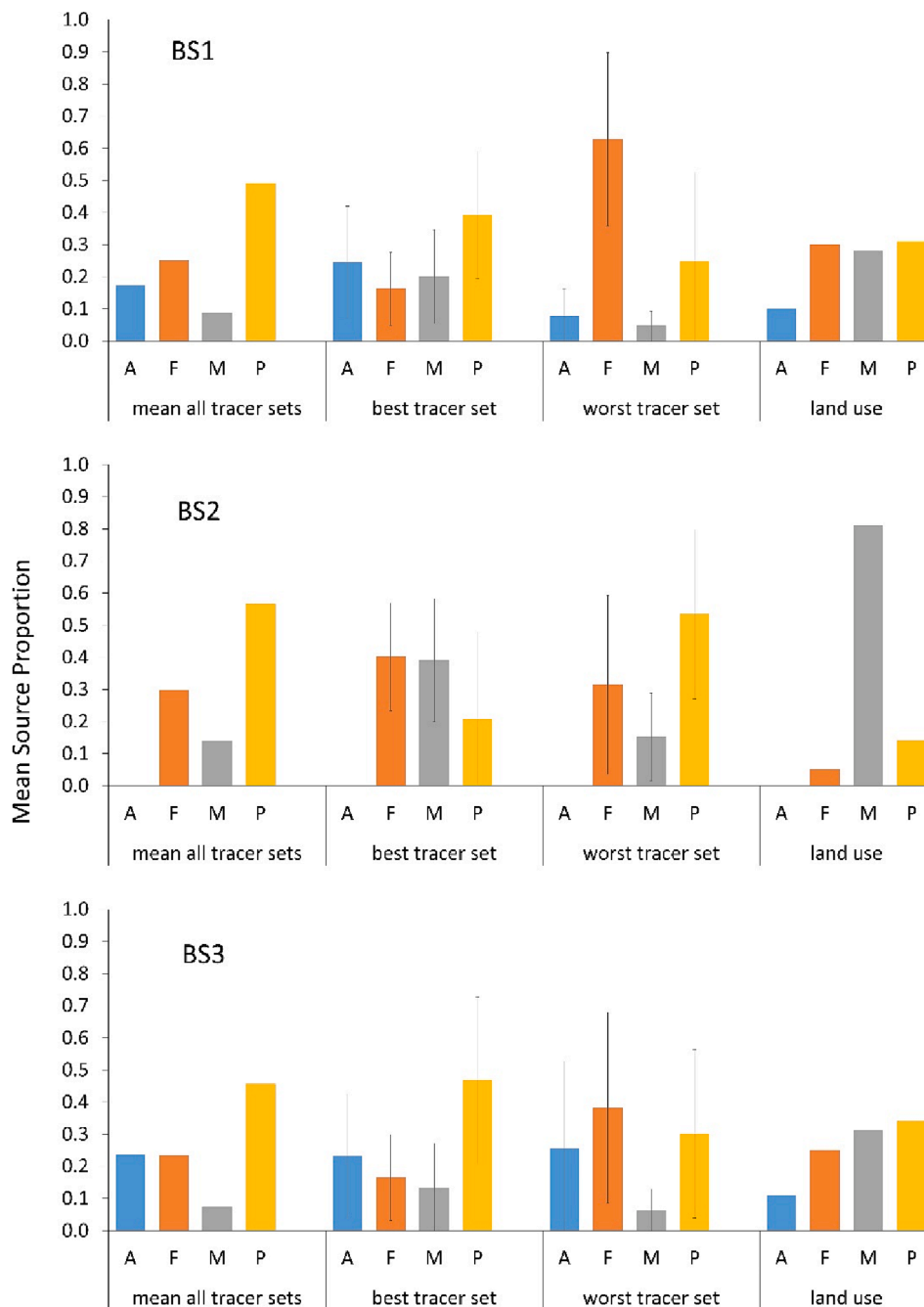

Fig. 11. Mean source proportion of four land use sources (arable, forest, moorland and pasture) modelled using sediment fingerprinting (n-alkane ratios, and short chain (<C22) NLFA concentrations and CSSI signatures as tracers) and a Bayesian unmixing model (MixSIAR) for three streambed sediment samples (BS1, BS2 and BS3) – in each case this accompanied by the corresponding percentage land use cover for the sub-catchments of BS1, BS2 and BS3. Error bars are +/- 1SD.

3.6. Contribution of land use sources to catchment streambed sediments

Each tracer set was used to model the relative land use contribution to the three streambed sediment samples (BS1, BS2 (no arable land use present) and BS3) using MixSIAR (Fig. 11, Table 9). On average, at every streambed sample site, the land use with the smallest modelled source proportion was moorland (mean 0.09, 0.14 and 0.07 at sites BS1, BS2 and BS3 respectively) and the land use with the largest modelled source proportion was pasture land (mean 0.49, 0.57 and 0.46 at sites BS1, BS2 and BS3 respectively) (Table 9). In this study catchment, where discrimination between four different land uses was required, the combination of SC-NLFA concentrations + their CSSI signatures (Nlfa-Both) provided the most accurate "best" land use source discrimination based on their reproduction of known source apportionment. Conversely, the "worst" land use source discrimination was found when using the tracer set composed of both *n*-alkane ratios and *n*-alkane CSSI (NalkBoth). There is a marked difference between the source proportions modelled using the "best", "worst" and taking the "mean" of all the tracer sets (Fig. 11) and a different interpretation could be made of the relative contributions of the four land uses to the sediment in the streams from these different tracer sets. For example, the "best" tracer set predicts relatively similar source proportions from all the land uses (arable = 0.25, forest = 0.16, moorland = 0.20 and pasture = 0.39) at site BS1, whereas the "worst" tracer set predicts a dominant contribution from forest land (0.63), a moderate input from pasture land (0.25) and very little input from arable or moorland (0.08 and 0.05 respectively). These results suggest that fingerprinting methods using the output of unmixing models such as MixSIAR could be improved by the use of multiple tracer sets if there is a commensurate way to determine which tracer set provides the "best" capacity for land use source discrimination. In this study, the use of virtual mixtures offered a way to select which tracers provided the best capacity for land use source discrimination by reproducing known source apportionments. The best estimates for source apportionment for the four land uses were arable = 0.25, forest = 0.16, moorland = 0.20 and pasture = 0.39 at BS1, forest = 0.40, moorland = 0.39 and pasture = 0.21 at BS2 (no arable land), and arable = 0.23, forest = 0.17, moorland = 0.13 and pasture = 0.47 at BS3 (Fig. 11).

Arable land use covered approximately 10% of the BS3 catchment area and also of the sub-catchment relating to BS1 (Fig. 11). At both BS1 and BS3, arable land made a larger contribution to the streambed sediments than would be expected given the amount of arable land within those sub-catchments. For ca. 400 m upstream of BS1 the stream passes through arable land, some of which is located on steeper slopes (>5°), which could have led to a locally higher level of erosion and input of arable soil to the stream (Wischmeier and Smith, 1978). Similarly, Pulley and Collins (2018) found sediment sources in close proximity to their sediment sampling locations were of the greatest importance in their SF study in a UK agricultural catchment, and Lei et al. (2021) found that concentrations of nutrients in streams were intensified by steeper slopes in agricultural and pasture fields in Germany. These results support other studies that have found arable land makes a larger contribution to river sediments than would be predicted from the proportion of land that it covers within a catchment (Wang et al., 2021).

At streambed sites BS1 and BS3 30% and 25% of the respective sub-catchment land is covered in forest, however forest land contributed only 13% and 17% respectively to the streambed sediments. The proportion of sediment originating from forest land in this catchment is not high but is higher than that for a similar study carried out in another Aberdeenshire catchment (Tarland; Hirave et al., 2020a) which found minimal inputs from forest land uses to the headwater stream suspended sediment flux (ca. 2%) attributed to high canopy cover and a dense organic layer on the soil surface resulting in low erosion rates. Wang et al. (2021) also found the contributions from forest and moorland to riverbed sediments were considerably smaller than those from arable land (forest 8% and moorland 6%: cf. arable 45%). Forest accounts for<5% of the land cover in the sub-catchment at BS2 but contributed 40% of the streambed OC. The forest land in the BS2 sub-catchment is located on land at low risk of erosion (Lilly and Baggaley, 2018), however, all forest land is in close proximity to BS2, suggesting that these proximal areas had a large influence on the composition of streambed sediments, possibly through direct input of woody material to the stream (Lavrieux et al., 2019; Wiltshire et al., 2022).

When considering BS3, located at the catchment outlet, nearly 30% percent of the catchment land cover is moorland, however, the MixSIAR model predicted a proportional contribution of only 0.13 from moorland. Similarly, at BS2 moorland encompasses nearly 80% of the land cover respectively but made a smaller contribution to the streambed sediments (proportion 0.39). Moorland covers large areas of the Loch Davan catchment and is located on the steepest slopes (Fig. 1c) in areas at higher erosion risk (Lilly and Baggaley, 2018). The erosion risk map covering this catchment (Lilly and Baggaley, 2018) was constructed by estimating the risk of a bare soil being eroded under intense or prolonged rainfall, with steeper slopes leading to faster runoff. The minimal input of moorland soil to the streambed sediments suggests that despite their location on steep slopes the vegetation cover found on these moorlands makes this land use relatively resistant to soil erosion. Hirave et al., (2020a) also found that moorland contributed marginally to suspended stream sediments (<2%), despite covering 16% of the catchment area, which they attributed to the thick organic layer covering the soil surface for this land use resulting in less erodibility of the soil.

At each streambed site there was a larger contribution from pasture land to the streambed sediments (BS1 0.39, BS2 0.21 and BS3 0.47 respectively: Fig. 11) than would be expected given the amount of pasture land within those sub-catchments (30%, 14% and 30% respectively). The results of this study are consistent with those of other studies that found a high contribution (annual average 56–79%) of permanent grasslands to the suspended sediments and higher soil erosion rate estimates from improved grassland (as compared to extensive arable land use), for other areas in Scotland (Hirave et al., 2020a; Rickson et al., 2019).

4. Conclusion

Building on previous research that has shown SC-NFLA hold promise for distinguishing land use origins of recently eroded sediment, specifically when there is land use change, the collection of new empirical

Table 9
Mean, minimum and maximum relative land use contribution to the three streambed sediment samples (BS1, BS2 (no arable land use present) and BS3) using MixSIAR and tracers sets a) n-alkane ratios alone (Nalk), b) n-alkane ratios + CSSI signatures (NalkBoth), c) n-alkane ratios + SC-NLFA concentrations (NalkNlfa), d) Scenario c + SC-NLFA CSSI signatures (NalkNlfaBoth), e) SC-NLFA concentrations only (Nlfa), f) SC-NLFA concentrations + CSSI signatures (NlfaBoth), and g) all tracers.

	BS1			BS2			BS3		
	mean	min	max	mean	min	max	mean	min	max
arable	0.17	0.07	0.26				0.24	0.16	0.38
forest	0.25	0.11	0.63	0.30	0.12	0.56	0.23	0.06	0.38
moorland	0.09	0.04	0.21	0.14	0.05	0.39	0.07	0.04	0.13
pasture	0.49	0.25	0.73	0.57	0.21	0.83	0.46	0.30	0.74

data and novel combinations of biomarkers in this study found that land use can be distinguished more accurately in organic sediment finger-printing when combining *n*-alkanes and SC-NLFA or using SC-NLFA and their CSSI alone. There was a marked difference between the source proportions modelled using different tracer sets (Fig. 11) with correspondingly different interpretations of the relative contributions of the four land uses to the sediment in the streams. These results suggest that fingerprinting methods using the output of unmixing models such as MixSIAR could be improved by the use of multiple tracer sets if there is a corresponding way to determine which tracer set provides the "best" capacity for land use source discrimination. The use of virtual mixtures and different combinations of tracers offer a way to select tracers with the best capacity for land use source discrimination by reproducing known source apportionments and a more reliable "best" estimate of the proportional contribution of each land use to the catchment streambed sediments. In this study a 50/50 ratio was selected for the virtual mixtures to assess which tracer set performed best on average for all the individual source combinations without having to make assumptions about what the likely source proportions would be. In future studies, varying "known" contributions (from the 50/50 ratio used in the virtual mixtures in this study) could give additional information on the combined tracer set/mixing model performance at more "extreme" source ratios.

This new contribution to the organic sediment fingerprinting field highlights that different combinations of biomarkers may be required to optimise discrimination between soils from certain land use sources (e. g., arable-pasture). The use of virtual mixtures, as presented in this study, provides a method to determine if addition or removal of tracers can improve relative error in source discrimination. Further studies are required to determine whether different sets of biomarkers (*n*-alkane, SC-NLFA, concentrations, CSSI δ^{13}C signatures) are consistent in better distinguishing between certain land use combinations (e.g., arable-pasture) in varied geographical areas. Combining SOC biomarkers representing different soil communities could have a significant impact on the identification of recent sources of sediment within catchments and therefore on the development of effective management strategies.

Declaration of Competing Interest

The authors declare that they have no known competing financial interests or personal relationships that could have appeared to influence the work reported in this paper.

Data availability

Data will be made available on request.

Acknowledgements

References

Addy, S., Ghimire, S., Cooksley, S., 2012. Assessment of the multiple benefits of river restoration: the Logie Burn meander reconnection project. BHS Elev. Natl. Symp. Hydrol. a Chang. world, Dundee 2012 01–05. 10.7558/bhs.2012.ns01.

Alewell, C., Birkholz, A., Meusburger, K., Schindler Wildhaber, Y., Mabit, L., 2016. Quantitative sediment source attribution with compound-specific isotope analysis in a C3 plant-dominated catchment (central Switzerland). Biogeosciences 13, 1587–1596. https://doi.org/10.5194/bg-13-1587-2016.

Ankit, Y., Muneer, W., Gaye, B., Lahajnar, N., Bhattacharya, S., Bulbul, M., Jehangir, A., Anoop, A., Mishra, P.K., 2022. Apportioning sedimentary organic matter sources and its degradation state- Inferences based on aliphatic hydrocarbons amino acids and δ15N. Environ. Res. 205, 112409. https://doi.org/10.1016/j.envres.2021.112409.

Barka, E.A., Vatsa, P., Sanchez, L., Nathalie Gaveau-Vaillant, C.J., Klenk, H.-P., Clément, C., Ouhdouch, Y., van Wezeld, G.P., 2016. Taxonomy, physiology, and natural products of actinobacteria. Am. Soc. Microbiol. 80, 1–43. https://doi.org/10.1128/MMBR.00019-15.Address.

Battin, T.J., Luyssaert, S., Kaplan, L.A., Aufdenkampe, A.K., Richter, A., Tranvik, L.J., 2009. The boundless carbon cycle. Nat. Geosci. 2, 598–600. https://doi.org/10.1038/ngeo618.

Blake, W.H., Ficken, K.J., Taylor, P., Russell, M.A., Walling, D.E., 2012. Tracing crop-specific sediment sources in agricultural catchments. Geomorphology 139–140, 322–329. https://doi.org/10.1016/j.geomorph.2011.10.036.

Bush, R.T., McInerney, F.A., 2013. Leaf wax n-alkane distributions in and across modern plants: Implications for paleoecology and chemotaxonomy. Geochim. Cosmochim. Acta 117, 161–179. https://doi.org/10.1016/j.gca.2013.04.016.

Chen, F.X., Fang, N.F., Wang, Y.X., Tong, L.S., Shi, Z.H., 2017. Biomarkers in sedimentary sequences: Indicators to track sediment sources over decadal timescales. Geomorphology 278, 1–11. https://doi.org/10.1016/j.geomorph.2016.10.027.

Chen, Y., Wang, Y., Yu, K., Zhao, Z., Lang, X., 2022. Occurrence characteristics and source appointment of polycyclic aromatic hydrocarbons and n-alkanes over the past 100 years in southwest China. Sci. Total Environ. 808, 151905 https://doi.org/10.1016/j.scitotenv.2021.151905.

Chikaraishi, Y., Naraoka, H., 2003. Compound-specific δD-δ13C analyses of n-alkanes extracted from terrestrial and aquatic plants. Phytochemistry 63 (3), 361–371. https://doi.org/10.1016/S0031-9422(02)00749-5.

Cole, B., King, S., Ogutu, B., Palmer, D., Smith, G., Balzter, H., 2015. Corine land cover 2012 for the UK, Jersey and Guernsey [WWW Document]. NERC Environ. Inf. Data Cent. URL 10.5285/32533dd6-7c1b-43e1-b892-e80d61a5ea1d (accessed 1.18.21).

Collins, A.L., Blackwell, M., Boeckx, P., Chivers, C.A., Emelko, M., Evrard, O., Foster, I., Gellis, A., Gholami, H., Granger, S., Harris, P., Horowitz, A.J., Laceby, J.P., Martinez-Carreras, N., Minella, J., Mol, L., Nosrati, K., Pulley, S., Silins, U., da Silva, Y.J., Stone, M., Tiecher, T., Upadhayay, H.R., Zhang, Y., 2020. Sediment source fingerprinting: benchmarking recent outputs, remaining challenges and emerging themes. J. Soils Sediments. https://doi.org/10.1007/s11368-020-02755-4.

Cooper, R.J., Pedentchouk, N., Hiscock, K.M., Disdle, P., Krueger, T., Rawlins, B.G., 2015. Apportioning sources of organic matter in streamed sediments: an integrated molecular and compound-specific stable isotope approach. Sci. Total Environ. 520, 187–197. https://doi.org/10.1016/j.scitotenv.2015.03.058.

Cranwell, P.A., 1981. Diagenesis of free and bound lipids in terrestrial detritus deposited in a lacustrine sediment. Org. Geochem. 3, 79–89. https://doi.org/10.1016/0146-6380(81)90002-4.

Dominati, E., Patterson, M., Mackay, A., 2010. A framework for classifying and quantifying the natural capital and ecosystem services of soils. Ecol. Econ. 69, 1858–1868. https://doi.org/10.1016/j.ecolecon.2010.05.002.

Dove, H., Mayes, R.W., 2006. Protocol for the analysis of n-alkanes and other plant-wax compounds and for their use as markers for quantifying the nutrient supply of large mammalian herbivores. Nat. Protoc. 1, 1680–1697. https://doi.org/10.1038/nprot.2006.225.

Fang, J., Wu, F., Xiong, Y., Li, F., Du, X., An, D., Wang, L., 2014. Source characterization of sedimentary organic matter using molecular and stable carbon isotopic composition of n-alkanes and fatty acids in sediment core from Lake Dianchi, China. Sci. Total Environ. 473–474, 410–421. https://doi.org/10.1016/j.scitotenv.2013.10.066.

Fatahi, A., Gholami, H., Esmaeilpour, Y., Fathabadi, A., 2022. Fingerprinting the spatial sources of fine-grained sediment deposited in the bed of the Mehran River, southern Iran. Sci. Rep. 12, 1–17. https://doi.org/10.1038/s41598-022-07882-1.

Fenton, N., Neil, M., 2018. Risk Assessment and Decision Analysis with Bayesian Networks. CRC Press Taylor & Francis, Boca Raton, Florida, USA.

Ferlian, O., Cesarz, S., Marhan, S., Scheu, S., 2014. Carbon food resources of earthworms of different ecological groups as indicated by 13C compound-specific stable isotope analysis. Soil Biol. Biochem. 77, 22–30. https://doi.org/10.1016/j.soilbio.2014.06.002.

Ferrari, A.E., Ravnskov, S., Larsen, J., Tønnersen, T., Maronna, R.A., Wall, L.G., 2015. Crop rotation and seasonal effects on fatty acid profiles of neutral and phospholipids extracted from no-till agricultural soils. Soil Use Manag. 31, 165–175. https://doi.org/10.1111/sum.12165.

Ficken, K.J., Li, B., Swain, D.L., Eglinton, G., 2000. An n-alkane proxy for the sedimentary input of submerged/floating freshwater aquatic macrophytes. Org. Geochem. 31, 745–749. https://doi.org/10.1016/S0146-6380(00)00081-4.

Galoski, C.E., Jiménez Martínez, A.E., Schultz, G.B., dos Santos, I., Froehner, S., 2019. Use of n-alkanes to trace erosion and main sources of sediments in a watershed in southern Brazil. Sci. Total Environ. 682, 447–456. https://doi.org/10.1016/j.scitotenv.2019.05.209.

Gibbs, M.M., 2008. Identifying source soils in contemporary estuarine sediments: a new compound-specific isotope method. Estuaries and Coasts 31, 344–359. https://doi.org/10.1007/s12237-007-9012-9.

Glaser, B., Zech, W., 2005. Reconstruction of climate and landscape changes in a high mountain lake catchment in the Gorkha Himal, Nepal during the Late Glacial and Holocene as deduced from radiocarbon and compound-specific stable isotope

analysis of terrestrial, aquatic and microbi. Org. Geochem. 36, 1086–1098. https://doi.org/10.1016/j.orggeochem.2005.01.015.

Glendell, M., Jones, R., Dungait, J.A.J., Meusburger, K., Schwendel, A.C., Barclay, R., Barker, S., Haley, S., Quine, T.A., Meersmans, J., 2018. Tracing of particulate organic C sources across the terrestrial-aquatic continuum, a case study at the catchment scale (Carminowe Creek, southwest England). Sci. Total Environ. 616, 1077–1088. https://doi.org/10.1016/j.scitotenv.2017.10.211.

Gobin, A., Jones, R., Kirkby, M., Campling, P., Govers, G., Kosmas, C., Gentile, A.R., 2004. Indicators for pan-European assessment and monitoring of soil erosion by water. Environ. Sci. Policy 7, 25–38. https://doi.org/10.1016/j.envsci.2003.09.004.

Griepentrog, M., Bodé, S., Boeckx, P., Wiesenberg, G.L.B., 2016. The fate of plant wax lipids in a model forest ecosystem under elevated CO_2 concentration and increased nitrogen deposition. Org. Geochem. 98, 131–140. https://doi.org/10.1016/j.orggeochem.2016.05.005.

Grimalt, J.O., Torras, E., Albaigés, J., 1988. Bacterial reworking of sedimentary lipids during sample storage. Org. Geochem. 13, 741–746. https://doi.org/10.1016/0146-6380(88)90096-4.

Hancock, G.J., Revill, A.T., 2013. Erosion source discrimination in a rural Australian catchment using compound-specific isotope analysis (CSIA). Hydrol. Process. 27, 923–932. https://doi.org/10.1002/hyp.9466.

Haubert, D., Häggblom, M.M., Langel, R., Scheu, S., Ruess, L., 2006. Trophic shift of stable isotopes and fatty acids in Collembola on bacterial diets. Soil Biol. Biochem. 38, 2004–2007. https://doi.org/10.1016/j.soilbio.2005.11.031.

He, D., Ladd, S.N., Saunders, C.J., Mead, R.N., Jaff, R., 2020. Distribution of n-alkanes and their δ2H and δ13C values in typical plants along a terrestrial-coastal-oceanic gradient. Geochim. Cosmochim. Acta 281, 31–52.

Hemkemeyer, M., Dohrmann, A.B., Christensen, B.T., Tebbe, C.C., 2018. Bacterial preferences for specific soil particle size fractions revealed by community analyses. Front. Microbiol. 9, 1–13. https://doi.org/10.3389/fmicb.2018.00149.

Hemkemeyer, M., Christensen, B.T., Tebbe, C.C., Hartmann, M., 2019. Taxon-specific fungal preference for distinct soil particle size fractions. Eur. J. Soil Biol. 94, 103103 https://doi.org/10.1016/j.ejsobi.2019.103103.

Hirave, P., Glendell, M., Birkholz, A., Alewell, C., 2020a. Compound-specific isotope analysis with nested sampling approach detects spatial and temporal variability in the sources of suspended sediments in a Scottish mesoscale catchment. Sci. Total Environ., 142916 https://doi.org/10.1016/j.scitotenv.2020.142916.

Hirave, P., Wiesenberg, G.L.B., Birkholz, A., Alewell, C., 2020b. Understanding the effects of early degradation on isotopic tracers: implications for sediment source attribution using compound-specific isotope analysis (CSIA). Biogeosciences Discuss. 1–18 https://doi.org/10.5194/bg-2019-205.

Jeng, W.L., 2006. Higher plant n-alkane average chain length as an indicator of petrogenic hydrocarbon contamination in marine sediments. Mar. Chem. 102, 242–251. https://doi.org/10.1016/j.marchem.2006.05.001.

Jenkins, D. (Ed.), 1985. The biology and management of the River Dee. Institute of Terrestrial Ecology.

Koch, A., McBratney, A., Adams, M., Field, D., Hill, R., Crawford, J., Minasny, B., Lal, R., Abbott, L., O'Donnell, A., Angers, D., Baldock, J., Barbier, E., Binkley, D., Parton, W., Wall, D.H., Bird, M., Bouma, J., Chenu, C., Flora, C.B., Goulding, K., Grunwald, S., Hempel, J., Jastrow, J., Lehmann, J., Lorenz, K., Morgan, C.L., Rice, C.W., Whitehead, D., Young, I., Zimmermann, M., 2013. Soil security: solving the global soil crisis. Glob. Policy 4, 434–441. https://doi.org/10.1111/1758-5899.12096.

Lachance, C., Lobb, D.A., Pelletier, G., Thériault, G., Chrétien, F., 2020. Determination of sediment sources in a mixed watershed within the Appalachian-St. Lawrence Lowland Regions of southern Quebec using sediment fingerprinting. Environ. Monit. Assess. 192 https://doi.org/10.1007/s10661-020-08568-9.

Ladygina, N., Dedyukhina, E.G., Vainshtein, M.B., 2006. A review on microbial synthesis of hydrocarbons. Process Biochem. 41, 1001–1014. https://doi.org/10.1016/j.procbio.2005.12.007.

Lavrieux, M., Bréheret, J.G., Disnar, J.R., Jacob, J., Le Milbeau, C., Zocatelli, R., 2012. Preservation of an ancient grassland biomarker signature in a forest soil from the French Massif Central. Org. Geochem. 51, 1–10. https://doi.org/10.1016/j.orggeochem.2012.07.003.

Lavrieux, M., Birkholz, A., Meusburger, K., Wiesenberg, G.L.B., Gilli, A., Stamm, C., Alewell, C., 2019. Plants or bacteria? 130 years of mixed imprints in Lake Baldegg sediments (Switzerland), as revealed by compound-specific isotope analysis (CSIA) and biomarker analysis. Biogeosciences 16, 2131–2146. https://doi.org/10.5194/bg-16-2131-2019.

Lei, C., Wagner, P.D., Fohrer, N., 2021. Effects of land cover, topography, and soil on stream water quality at multiple spatial and seasonal scales in a German lowland catchment. Ecol. Indic. 120, 106940 https://doi.org/10.1016/j.ecolind.2020.106940.

Lilly, A., Baggaley, N.J., 2018. Soil erosion risk map of Scotland.

Liu, C., Hu, B.X., Li, Z., Yu, L., Peng, H., Wang, D., Huang, X., 2021a. Linking soils and streams: chemical composition and sources of eroded organic matter during rainfall events in a Loess hilly-gully region of China. J. Hydrol. 600, 126518 https://doi.org/10.1016/j.jhydrol.2021.126518.

Liu, C., Wu, Z., Hu, B.X., Li, Z., 2021b. Linking recent changes in sediment yields and aggregate-associated organic matter sources from a typical catchment of the Loess Plateau, China. Agric. Ecosyst. Environ. 321, 107606 https://doi.org/10.1016/j.agee.2021.107606.

Lizaga, I., Gaspar, L., Blake, W.H., Latorre, B., Navas, A., 2019. Fingerprinting changes of source apportionments from mixed land uses in stream sediments before and after an exceptional rainstorm event. Geomorphology 341, 216–229. https://doi.org/10.1016/j.geomorph.2019.05.015.

Lu, Y.H., Canuel, E.A., Bauer, J.E., Chambers, R.M., 2014. Effects of watershed land use on sources and nutritional value of particulate organic matter in temperate headwater streams. Aquat. Sci. 76, 419–436. https://doi.org/10.1007/s00027-014-0344-9.

McBratney, A., Field, D.J., Koch, A., 2014. The dimensions of soil security. Geoderma 213, 203–213. https://doi.org/10.1016/j.geoderma.2013.08.013.

Met Office, 2021. UK Climate Average [WWW Document]. URL https://www.metoffice.gov.uk/research/climate/maps-and-data/uk-climate-averages/gfjuxqwcs (accessed 1.18.21).

Meyers, P.A., 2003. Application of organic geochemistry to paleolimnological reconstruction: a summary of examples from the Laurention Great Lakes. Org. Geochem. 34, 261–289. https://doi.org/10.1016/S0146-6380(02)00168-7.

Nitzsche, K.N., Kleeberg, A., Hoffmann, C., Merz, C., Premke, K., Gessler, A., Sommer, M., Kayler, Z.E., 2022. Kettle holes reflect the biogeochemical characteristics of their catchment area and the intensity of the element-specific input. J. Soils Sediments 994–1009. https://doi.org/10.1007/s11368-022-03145-8.

Olsson, P.A., Van Aarle, I.M., Gavito, M.E., Bengtson, P., Bengtsson, G., 2005. 13C incorporation into signature fatty acids as an assay for carbon allocation in arbuscular mycorrhiza. Appl. Environ. Microbiol. 71, 2592–2599. https://doi.org/10.1128/AEM.71.5.2592-2599.2005.

Ordnance Survey, 2021. OS Terrain 5 [ASC geospatial data], Scale 1:10000, Tiles: nj30ne,nj30nw,nj30se,nj30sw,nj31se,nj31sw,nj40ne,nj40nw,nj40se,nj40sw,nj41se, nj41sw,nj50ne,nj50nw,nj50se,nj50sw,nj51se,nj51sw,no39ne,no39nw,no49ne, no49nw,no59ne,no59nw, [WWW Document]. EDINA Digimap Ordnance Surv. Serv. URL https://digimap.edina.ac.uk (accessed 12.14.18).

Owens, P.N., Batalla, R.J., Collins, A.J., Gomez, B., Hicks, D.M., Horowitz, A.J., Kondolf, G.M., Marden, M., Page, M.J., Peacock, D.H., Petticrew, E.L., Salomons, W., Trustrum, N.A., 2005. Fine-grained sediment in river systems: environmental significance and management issues. River Res. Appl. 21, 693–717. https://doi.org/10.1002/rra.878.

Owens, P.N., Blake, W.H., Gaspar, L., Gateuille, D., Koiter, A.J., Lobb, D.A., Petticrew, E. L., Reiffarth, D.G., Smith, H.G., Woodward, J.C., 2016. Fingerprinting and tracing the sources of soils and sediments: earth and ocean science, geoarchaeological, forensic, and human health applications. Earth-Science Rev. 162, 1–23. https://doi.org/10.1016/j.earscirev.2016.08.012.

Palazón, L., Latorre, B., Gaspar, L., Blake, W.H., Smith, H.G., Navas, A., 2015. Comparing catchment sediment fingerprinting procedures using an auto-evaluation approach with virtual sample mixtures. Sci. Total Environ. 532, 456–466. https://doi.org/10.1016/j.scitotenv.2015.05.003.

Phillips, D.L., Gregg, J.W., 2003. Source partitioning using stable isotopes: coping with too many sources. Oecologia 136, 261–269. https://doi.org/10.1007/s00442-003-1218-3.

Pulley, S., Collins, A.L., 2018. Tracing catchment fine sediment sources using the new SIFT (SedIment Fingerprinting Tool) open source software. Sci. Total Environ. 635, 838–858. https://doi.org/10.1016/j.scitotenv.2018.04.126.

Puttock, A., Dungait, J.A.J., Macleod, C.J.A., Bol, R., Brazier, R.E., 2014. Organic carbon from dryland soils. J. Geophys. Res. Biogeosciences 119, 2345–2357. https://doi.org/10.1002/2014JG002635.

R Core Team, 2020. R: A language and environment for statistical computing.

Ranjan, R.K., Routh, J., Val Klump, J., Ramanathan, A.L., 2015. Sediment biomarker profiles trace organic matter input in the Pichavaram mangrove complex, southeastern India. Mar. Chem. 171, 44–57. https://doi.org/10.1016/j.marchem.2015.02.001.

Rickson, R.J., Baggaley, N., Deeks, L.K., Graves, A., Hannam, J., Keay, C., Lilly, A., 2019. Developing a method to estimate the costs of soil erosion in high- risk Scottish catchments. Report to the Scottish Government. Available online from https://www.gov.scot/ISBN/978-1-83960-754-7.

RStudio Team, 2018. RStudio: Integrated Development for R.

Scheurer, K., Alewell, C., Bänninger, D., Burkhardt-Holm, P., 2009. Climate and land-use changes affecting river sediment and brown trout in alpine countries-a review. Environ. Sci. Pollut. Res. 16, 232–242. https://doi.org/10.1007/s11356-008-0075-3.

SEPA, 2021. Water Classification Hub [WWW Document]. Scottish Environ. Prot. Agency. URL https://www.sepa.org.uk/data-visualisation/water-classification-hub/.

Singh, S.N., Kumari, B., Mishra, S., 2012. Microbial Degradation of Alkanes, in: Microbial Degradation of Xenobiotics. pp. 439–469. 10.1007/978-3-642-23789-8_17.

Sirjani, E., Mahmoodabadi, M., Cerdà, A., 2022. Sediment transport mechanisms and selective removal of soil particles under unsteady-state conditions in a sheet erosion system. Int. J. Sediment Res. 37, 151–161. https://doi.org/10.1016/j.ijsrc.2021.09.006.

Smeaton, C., Cui, X., Bianchi, T.S., Cage, A.G., Howe, J.A., Austin, W.E.N., 2021. The evolution of a coastal carbon store over the last millennium. Quat. Sci. Rev. 266, 107081 https://doi.org/10.1016/j.quascirev.2021.107081.

Smith, H.G., Karam, D.S., Lennard, A.T., 2018b. Evaluating tracer selection for catchment sediment fingerprinting. J. Soils Sediments 18, 3005–3019. https://doi.org/10.1007/s11368-018-1990-7.

Smith, A.A., Tetzlaff, D., Soulsby, C., 2018a. On the use of storage selection functions to assess time-variant travel times in lakes. Water Resour. Res. 54, 5163–5185. https://doi.org/10.1029/2017WR021242.

Stenfert Kroese, J., Batista, P.V.G., Jacobs, S.R., Breuer, L., Quinton, J.N., Rufino, M.C., 2020. Agricultural land is the main source of stream sediments after conversion of an African montane forest. Sci. Rep. 10, 14827. https://doi.org/10.1038/s41598-020-71924-9.

Stock, B.C., Semmens, B.X., 2016. MixSIAR GUI User Manual. Version 3.1. 10.5281/zenodo.1209993.

Stock, B.C., Jackson, A.L., Ward, E.J., Parnell, A.C., Phillips, D.L., Semmens, B.X., 2018. MixSIAR model description.

Stout, S.A., 2020. Leaf wax n-alkanes in leaves, litter, and surface soil in a low diversity, temperate deciduous angiosperm forest, Central Missouri, USA. Chem. Ecol. 810–826 https://doi.org/10.1080/02757540.2020.1789118.

Swales, A., Gibbs, M.M., 2020. Transition in the isotopic signatures of fatty-acid soil biomarkers under changing land use: insights from a multi-decadal chronosequence. Sci. Total Environ. 722, 137850 https://doi.org/10.1016/j.scitotenv.2020.137850.

Tekaya, M., Dahmen, S., Ben Mansour, M., Ferhout, H., Chehab, H., Hammami, M., Attia, F., Mechri, B., 2021. Foliar application of fertilizers and biostimulant has a strong impact on the olive (*Olea europaea*) rhizosphere microbial community profile and the abundance of arbuscular mycorrhizal fungi. Rhizosphere 19, 100402. https://doi.org/10.1016/j.rhisph.2021.100402.

Thornton, B., Zhang, Z., Mayes, R.W., Högberg, M.N., Midwood, A.J., 2011. Can gas chromatography combustion isotope ratio mass spectrometry be used to quantify organic compound abundance? Rapid Commun. Mass Spectrom. 25, 2433–2438. https://doi.org/10.1002/rcm.5148.

Torres, T., Ortiz, J.E., Martín-Sánchez, D., Arribas, I., Moreno, L., Ballesteros, B., Blázquez, A.N.A., Domínguez, J.A., Estrella, T.R., 2014. The long pleistocene record from the pego-oliva marshland (Alicante-Valencia, Spain). Geol. Soc. Spec. Publ. 388, 429–452. https://doi.org/10.1144/SP388.2.

Upadhayay, H.R., Bodé, S., Griepentrog, M., Huygens, D., Bajracharya, R.M., Blake, W. H., Dercon, G., Mabit, L., Gibbs, M., Semmens, B.X., Stock, B.C., Cornelis, W., Boeckx, P., 2017. Methodological perspectives on the application of compound-specific stable isotope fingerprinting for sediment source apportionment. J. Soils Sediments 17, 1537–1553. https://doi.org/10.1007/s11368-017-1706-4.

Upadhayay, H.R., Bodé, S., Griepentrog, M., Bajracharya, R.M., Blake, W., Cornelis, W., Boeckx, P., 2018. Isotope mixing models require individual isotopic tracer content for correct quantification of sediment source contributions. Hydrol. Process. 32, 981–989. https://doi.org/10.1002/hyp.11467.

Walling, D.E., Owens, P.N., Leeks, G.J.L., 1999. Fingerprinting suspended sediment sources in the catchment of the River Ouse, Yorkshire, UK. Hydrol. Process. 13, 955–975. https://doi.org/10.1002/(SICI)1099-1085(199905)13:7<955::AID-HYP784>3.0.CO;2-G.

Wang, X., Huang, X., Sachse, D., Hu, Y., Xue, J., Meyers, P.A., 2016. Comparisons of lipid molecular and carbon isotopic compositions in two particle-size fractions from surface peat and their implications for lipid preservation. Environ. Earth Sci. 75 https://doi.org/10.1007/s12665-016-5960-3.

Wang, X., Blake, W.H., Taylor, A., Kitch, J., Millward, G., 2021. Evaluating the effectiveness of soil conservation at the basin scale using floodplain sedimentary archives. Sci. Total Environ. 792, 148414 https://doi.org/10.1016/j.scitotenv.2021.148414.

Wang, Y., Yang, H., Zhang, J., Xu, M., Wu, C., 2015. Biomarker and stable carbon isotopic signatures for 100–200year sediment record in the Chaihe catchment in southwest China. Sci. Total Environ. 502, 266–275. https://doi.org/10.1016/j.scitotenv.2014.09.017.

Wiltshire, C., Glendell, M., Waine, T.W., Grabowski, R.C., Meersmans, J., 2022. Assessing the source and delivery processes of organic carbon within a mixed land use catchment using a combined n-alkane and carbon loss modelling approach. J. Soils Sediments. https://doi.org/10.1007/s11368-022-03197-w.

Wischmeier, W., Smith, D., 1978. Predicting rainfall erosion losses: a guide to conservation planning. Agricultural Handbook No. 537.

Xue, P.P., Carrillo, Y., Pino, V., Minasny, B., McBratney, A.B., 2018. Soil properties drive microbial community structure in a large scale transect in South Eastern Australia. Sci. Rep. 8, 1–11. https://doi.org/10.1038/s41598-018-30005-8.

Xue, Y., Chen, L., Zhao, Y., Feng, Q., Li, C., Wei, Y., 2022. Shift of soil fungal communities under afforestation in Nanliu River Basin, southwest China. J. Environ. Manage. 302, 114130 https://doi.org/10.1016/j.jenvman.2021.114130.

Yan, C., Zhang, Y., Zheng, M., Zhang, Y., Liu, M., Yang, T., Meyers, P.A., Huang, X., 2021. Effects of redox conditions and temperature on the degradation of Sphagnumn-alkanes. Chem. Geol. 561, 119927 https://doi.org/10.1016/j.chemgeo.2020.119927.

Zaitlin, B., Watson, S.B., Dixon, J., Steel, D., 2003. Actinomycetes in the Elbow River Basin, Alberta, Canada. Water Qual. Res. J. Canada 38, 115–125. https://doi.org/10.2166/wqrj.2003.007.

Zech, M., Buggle, B., Leiber, K., Marković, S., Glaser, B., Hambach, U., Huwe, B., Stevens, T., Sümegi, P., Wiesenberg, G., Zöller, L., 2009. Reconstructing Quaternary vegetation history in the Carpathian Basin, SE-Europe, using n-alkane biomarkers as molecular fossils: problems and possible solutions, potential and limitations. Quat. Sci. J. 58, 148–155. https://doi.org/10.3285/eg.58.2.03.

Zech, M., Pedentchouk, N., Buggle, B., Leiber, K., Kalbitz, K., Marković, S.B., Glaser, B., 2011. Effect of leaf litter degradation and seasonality on D/H isotope ratios of n-alkane biomarkers. Geochim. Cosmochim. Acta 75, 4917–4928. https://doi.org/10.1016/j.gca.2011.06.006.

Zech, M., Krause, T., Meszner, S., Faust, D., 2013. Incorrect when uncorrected: Reconstructing vegetation history using n-alkane biomarkers in loess-paleosol sequences - A case study from the Saxonian loess region, Germany. Quat. Int. 296, 108–116. https://doi.org/10.1016/j.quaint.2012.01.023.

Zhang, Y., Collins, A.L., McMillan, S., Dixon, E.R., Cancer-Berroya, E., Poiret, C., Stringfellow, A., 2017. Fingerprinting source contributions to bed sediment-associated organic matter in the headwater subcatchments of the River Itchen SAC, Hampshire, UK. River Res. Appl. 33, 1515–1526. https://doi.org/10.1002/rra.3172.

Zhang, Q., Liang, G., Zhou, W., Sun, J., Wang, X., He, P., 2016a. Fatty-acid profiles and enzyme activities in soil particle-size fractions under long-term fertilization. Soil Sci. Soc. Am. J. 80, 97–111. https://doi.org/10.2136/sssaj2015.07.0255.

Zhang, X., Gu, Q., Long, X.E., Li, Z.L., Liu, D.X., Ye, D.H., He, C.Q., Liu, X.Y., Väänänen, K., Chen, X.P., 2016b. Anthropogenic activities drive the microbial community and its function in urban river sediment. J. Soils Sediments 16, 716–725. https://doi.org/10.1007/s11368-015-1246-8.